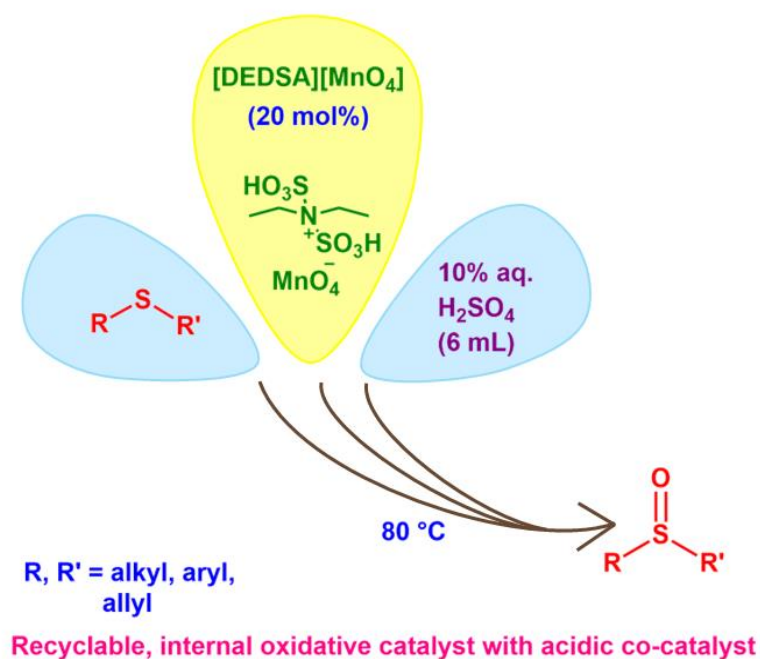


## Chapter 4

---

### *Functionalized Ammonium-Based Permanganate Hybrids as Sustainable Oxidative Catalysts for Selective Conversion of Organic Sulfides to Sulfoxides*



---

## Synopsis

In this chapter, two organic-inorganic hybrids of permanganate anions namely N, N'-diethyldisulfoammonium permanganate [DEDSA][MnO<sub>4</sub>] and 1,4-disulfopiperazinium permanganate [DSPZ][MnO<sub>4</sub>]<sub>2</sub> were developed as thermally stable oxidants through ion-exchange reactions of [DEDSA]Cl and [DSPZ].2Cl organic salts, respectively, with KMnO<sub>4</sub> at room temperature. Structural compositions and morphologies of both the hybrids were confirmed by various spectroscopic and analytical techniques like FT-IR, PXRD, Raman, UV-Vis DRS, SEM and EDX images. Comparative thermogravimetric analyses (TGA) with reference to the parent organic chloride salts expressed substantial changes in their thermal stabilities as well as hydrophilic/hydrophobic properties. The synthesized hybrids were employed as recyclable homogeneous oxidative catalysts for selective formation of sulfoxides from organic sulfides in 10% aqueous sulfuric solution at 80 °C with decent to excellent yields.

### 4.1. Introduction

Sulfide oxidation is an industrially important organic reaction to prepare sulfoxide and sulfone as key intermediates towards the development of a wide variety of value added chemical and biological products [1-6]. Most chiral sulfoxides or sulfones are widely used as auxiliaries in asymmetric synthesis that possess high biological activity [7, 8] or as ligands in the formation of metal complexes [9]. Likewise, allylic sulfoxides [10] and cyclic sulfoxides/sulfones are utilized as reaction intermediates for designing drug molecules [11]. Furthermore, dimethyl sulfoxide is extensively utilized as reaction medium and analytical solvent as well as multipurpose reactant [12, 13]. It has been observed that oxidative desulfurization of sterically hindered organic sulphide such as 4,6-dimethyldibenzothiophene (4,6-DMDBT) present in transportation fuel could be performed in mild conditions [14-16], as compared to severe reaction conditions employed in hydrodesulfurization reaction [17] which include consumption of excess hydrogen gas at high pressure (approx. 50-100 bar) and temperature (around 643 K) with notable increase of operational cost. Many reported methods of sulfide oxidations are not satisfactory with stoichiometric amounts of reagents because of unfavourable over-oxidized by-products formation and thus make them unfit for large-scale syntheses [18-21]. So, it is very essential to develop catalytic route of sulfide oxidation involving

---

environmentally benign oxidants, catalysts and solvent to reduce different limitations of traditional reagents of sulfide oxidation [18].

Few environmentally benign oxidative systems have been developed for sulfide oxidation using hydrogen peroxide as a greener oxidant in ionic liquids and produced sulfoxide selectively under mild reaction conditions [22-23, 17]. Some metal containing organic salts, particularly the polyoxometalate hybrids of organic cations, were also investigated as recyclable and selective oxidative catalysts for sulfide oxidation [24-29]. Among varied types of metal-based oxidants [30-33], potassium permanganate is known to be an effective oxidant in organic chemistry for its easy availability and cost-efficiency [34]. Non-selective sulfide oxidation was reported by Bordwell *et al.* with excess amount of  $\text{KMnO}_4$  in basic aqueous solution [35]. Few reports revealed mechanistic and kinetic study of the sulfide oxidation with excess amount of the  $\text{KMnO}_4$  in basic solution to get moderate yields of the oxidized products [36, 37]. The effect of solvents on product selectivity of sulfide oxidation using permanganate anion was reported by Shaabani *et al.* [38], as mentioned in **Chapter 1A, sub-unit 1A.5.2**. To know the exact mechanism of sulfide oxidation by  $\text{KMnO}_4$ , computational study was also performed by Arumugam *et al.* [39]. The literature of sulfide oxidation as included in **Chapter 1A (sub-unit 1A.5.2)** showed development of solid supported reagents of  $\text{KMnO}_4$  in presence of different support materials such as alumina,  $\text{MnO}_2$ , montmorillonite-K10,  $\text{MnSO}_4 \cdot \text{H}_2\text{O}$  with modification of the non-selective oxidative power of potassium permanganate [40-43]. All these supported reagents took longer reaction periods (1-20 h), despite the use of excess amount of oxidants.

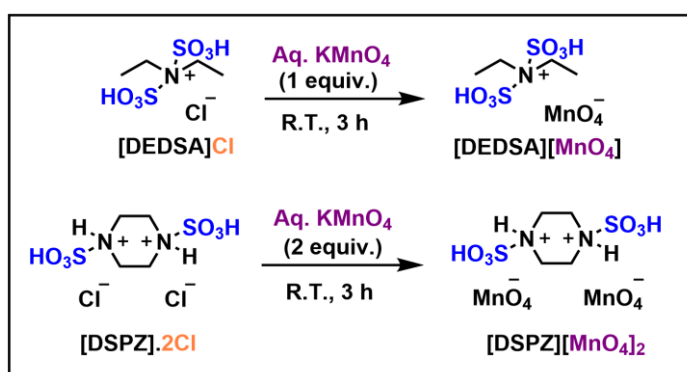
As discussed in **the sub-unit 1A.5.2.**, eventually, the selective oxidation of organic sulfides to sulfones was also studied using highly unstable and freshly prepared organic-inorganic hybrid of permanganate oxidants [44], such as benzyltriethylammonium permanganate [45, 46], methyltriphenylphosphonium permanganate [47] and tetra-*n*-butylammonium permanganate [48] at lower temperature in organic solvents with careful handling due to their explosive nature. It was noticed that *N,N'*-dibenzyl-*N,N,N',N'*-tetramethyl diammonium permanganate (DBTMEP) was reported as a thermally stable oxidant up to 110 °C for the selective conversion of sulfides to sulfones [49], however, it decomposed violently on harsh grinding.

Considering the state of circumstances, a viable organic-inorganic hybrid of permanganate anion with organic cation could be synthesized by ion-exchange reaction of  $\text{N-SO}_3\text{H}$  functionalized cyclic/acyclic ammonium based ionic liquids of chloride anion

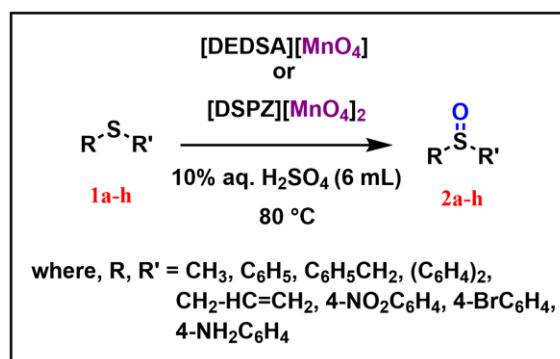
---

with permanganate anion of  $\text{KMnO}_4$ . It is well known that organic salts of organic or inorganic anions tethered with  $-\text{COOH}$ ,  $-\text{SO}_3\text{H}$  groups in organic cations have been developed as task-specific ionic liquids if their melting points exist below  $100\text{ }^\circ\text{C}$  and possess all the unique physicochemical properties of ionic liquids for further uses as functional materials in different fields [50-53]. By incorporating sulfonic groups into the organic cation of permanganate hybrid, one could expect strong electrostatic interactions between the ion-pair involving intra-molecular H-bonding interactions of  $-\text{OH}$  groups of sulfonic acid with the oxygen atoms of permanganate anion. In addition to that, the possible intermolecular H-bonding interactions between the cations of permanganate hybrids via sulfonic groups might tightly pack all molecules into rigid material with higher thermal stability.

Extending our previous works on catalytic performance of various organic-inorganic hybrids based on task-specific ionic liquids [54, 55], we focused on synthesizing a mono-cationic N, N'-diethyldisulfoammonium organic salt ( $[\text{DEDSA}]^+$ ) and a dicationic 1,4-disulfopiperazinium organic salt ( $[\text{DSPZ}]^{2+}$ ) with permanganate as anion according to **Scheme 4.1**. In both cases, the synthetic procedures involved ion-exchange between the reported precursor ionic liquid/salt ( $[\text{DEDSA}]\text{Cl}$  and  $[\text{DSPZ}]\cdot 2\text{Cl}$ ) and aqueous solution of potassium permanganate, respectively. After confirming the compositions of both hybrids using various analytical tools, their oxidizing capacities were explored as reusable homogeneous catalysts in the selective oxidation of organic sulfides to sulfoxides in aqueous solution of sulfuric acid under reflux conditions.



**Scheme 4.1:** Synthesis of permanganate hybrids of  $-\text{SO}_3\text{H}$  functionalized diethylammonium/piperazinium cations.



**Scheme 4.2:** Selective oxidation of sulfides to sulfoxides by the permanganate hybrids.

## 4.2. Results and discussion

### 4.2.1. Catalyst characterization

At first, two N-SO<sub>3</sub>H functionalized ammonium cation-based permanganate salts i.e. N, N'-diethyldisulfoammonium permanganate [DEDSA][MnO<sub>4</sub>] and 1,4-disulfo piperazinium permanganate [DSPZ][MnO<sub>4</sub>]<sub>2</sub> were prepared according to **Scheme 4.1** and then subjected to various analytical techniques to know their structural compositions as well as morphologies. Oxidative catalytic efficiencies of the synthesized hybrids were explored in the selective oxidation of organic sulfides in aqueous medium in presence of an acidic co-catalyst (**Scheme 4.2**).

#### 4.2.1.1. NMR and FT-IR analysis

In both synthesized sulfonic acid functionalized permanganate hybrids, the existence of organic cations was evidenced from <sup>1</sup>H and <sup>13</sup>C NMR spectra (**section 4.4.4**) of the precursor chloride based organic salts i.e. [DEDSA]Cl and [DSPZ].2Cl because of difficulties in solubilization of the permanganate hybrids of ammonium cations in most of the common NMR solvents. Furthermore, the comparative FT-IR spectra of synthesized materials to their respective precursor ionic liquid/salt showed the inclusion of organic cations as indicated by the characteristic vibrational peaks of sulfonic groups attached to both ammonium and piperazinium cations (**Fig. 4.1a and 4.1c**). In case of [DEDSA][MnO<sub>4</sub>] (**Fig. 4.1a**), the attached -SO<sub>3</sub>H groups showed prominent but overlapping S-O asymmetric and symmetric stretches at 1111 cm<sup>-1</sup> and 1028 cm<sup>-1</sup>, along with a sharp S-O bending vibration at 523 cm<sup>-1</sup> as compared to the same vibrations at 1128 cm<sup>-1</sup>, 1057 cm<sup>-1</sup> and 583 cm<sup>-1</sup>, respectively, for the parent ionic liquid [DEDSA]Cl [56]. The peaks at 712 cm<sup>-1</sup> and 1457 cm<sup>-1</sup> were associated to the out of plane ring bending

vibration of C-H bond and bending vibrations of  $-\text{CH}_2$  group, respectively [57]. A weak peak at  $830\text{ cm}^{-1}$  occurred due to stretching vibration of N-S bond. The physisorbed water molecules along with O-H stretch of  $-\text{SO}_3\text{H}$  groups caused a broad peak around  $3000\text{--}3500\text{ cm}^{-1}$ , while H-O-H bending vibration of physisorbed water gave rise to a medium strength peak at  $1628\text{ cm}^{-1}$ . Weak stretches around  $2800\text{--}2900\text{ cm}^{-1}$  were observed due to methyl group C-H stretch. The distinctive peak at  $910\text{ cm}^{-1}$  for  $\text{MnO}_4^-$  ion was found to be overlaying with the intense peak of  $[\text{DEDSA}][\text{MnO}_4]$  around  $1028\text{--}1111\text{ cm}^{-1}$  as IR active vibration, contrary to its inactive character in Raman spectra [Fig. 4.5c] of the hybrid [58, 59].

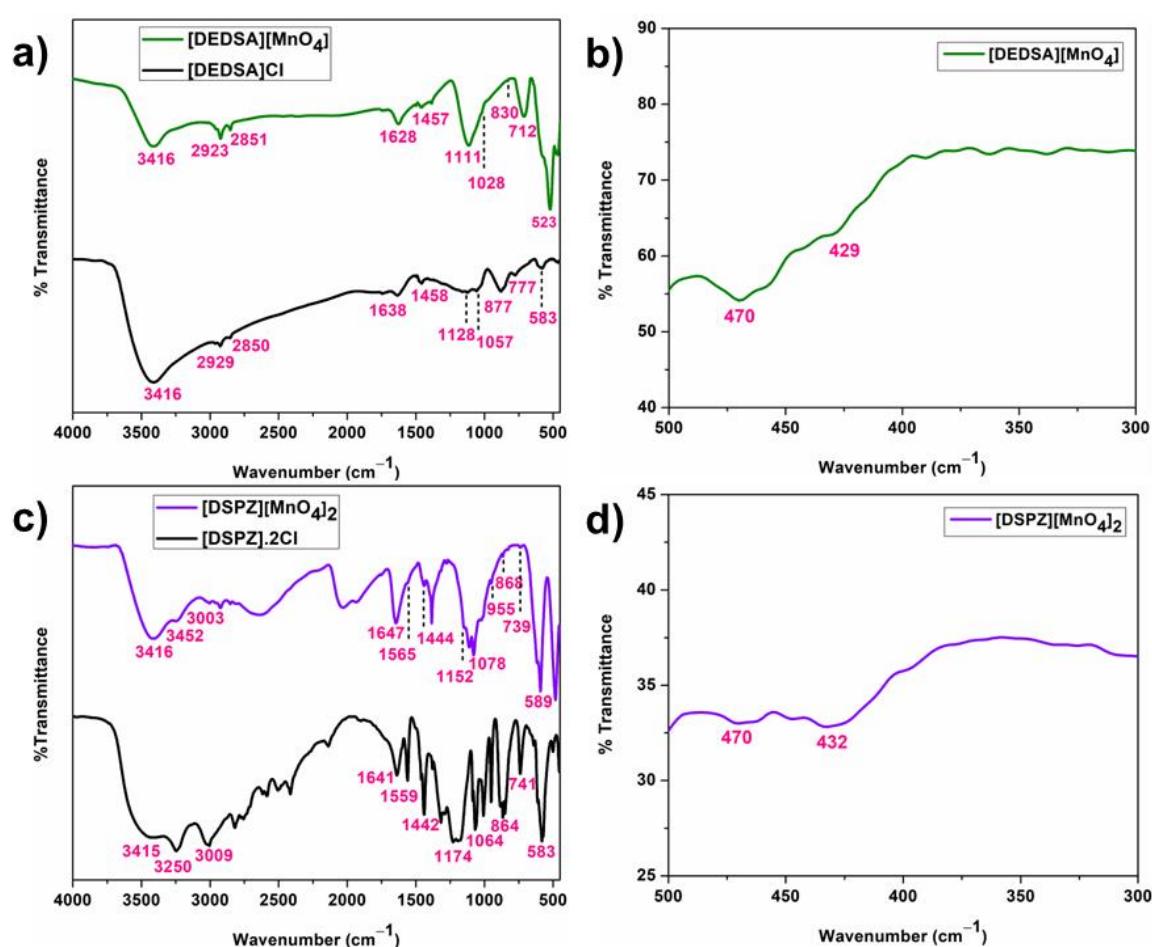


**Fig. 4.1:** Comparative FT-IR spectra of a)  $[\text{DEDSA}]\text{Cl}$  and  $[\text{DEDSA}][\text{MnO}_4]$ , b) Far-IR of  $[\text{DEDSA}][\text{MnO}_4]$ , c) Comparative FT-IR spectra of  $[\text{DSPZ}]\cdot 2\text{Cl}$  and  $[\text{DSPZ}][\text{MnO}_4]_2$ , d) Far-IR of  $[\text{DSPZ}][\text{MnO}_4]_2$ .

In the FT-IR spectrum of  $[\text{DSPZ}][\text{MnO}_4]_2$  in Fig. 4.1c, all the characteristic vibrations of sulfonic group such as S-O asymmetric, symmetric and bending vibrations were observed at  $1152\text{ cm}^{-1}$ ,  $1078\text{ cm}^{-1}$  and  $589\text{ cm}^{-1}$ , respectively, as compared to their

original positions in the precursor salt [DSPZ].2Cl at  $1174\text{ cm}^{-1}$ ,  $1064\text{ cm}^{-1}$  and  $583\text{ cm}^{-1}$ . It also showed a weak peak at  $868\text{ cm}^{-1}$  for N-S stretch in addition to two weak peaks at  $739\text{ cm}^{-1}$  for out of plane ring bending of C-H bond and at  $1444\text{ cm}^{-1}$  for  $\text{CH}_2$  groups bending vibrations of piperazine ring [57]. The sharp peak at  $1647\text{ cm}^{-1}$  was caused by bending vibrations of N-H bond, but the broad peaks around  $2700\text{--}3500\text{ cm}^{-1}$  could be due to the overlapped N-H bond stretch, C-H bond stretch and O-H bond stretching vibrations of  $-\text{SO}_3\text{H}$  groups along with intermolecular H-bonded  $\text{H}_2\text{O}$  molecules. The weak peak at  $955\text{ cm}^{-1}$  for  $\text{MnO}_4^-$  anion was observed in case of piperazinium permanganate hybrid, although it was absent in the Raman spectra of the hybrid (**Fig. 4.5d**). Additionally, Far-IR analysis showed the appearance of two weak vibrations around  $400\text{--}500\text{ cm}^{-1}$  in both materials, referring to  $\nu_4(\text{F}_2)$  Raman active mode of  $\text{MnO}_4^-$  [60], which also justified the inclusion of permanganate anion in the hybrids (**Fig. 4.1b** for [DEDSA][ $\text{MnO}_4$ ] and **Fig. 4.1d** for [DSPZ][ $\text{MnO}_4$ ]<sub>2</sub>).

#### 4.2.1.2. Thermogravimetric analysis

Thermogravimetric analysis (TGA) of [DEDSA][ $\text{MnO}_4$ ] in **Fig. 4.2a** expressed a greater hydrophobic nature than the parent ammonium chloride [DEDSA]Cl, as this hybrid did not lose any physisorbed water around  $100\text{ }^\circ\text{C}$ , contrary to its precursor [DEDSA]Cl, which lost around 14% of physisorbed water (equivalent to 2 molecules of water). Above  $150\text{ }^\circ\text{C}$ , the hybrid displayed around 2-4% mass loss up to  $600\text{ }^\circ\text{C}$  that could be attributed to elimination of crystallized water through cleavages of strong intermolecular H-bonding interactions involving the sulfonic groups of hybrids. In contrast, the precursor [DEDSA]Cl salt observed to be thermally stable only up to  $250\text{ }^\circ\text{C}$ . On the other hand, the comparative TGA plots of [DSPZ][ $\text{MnO}_4$ ]<sub>2</sub> with the precursor organic salt [DSPZ].2Cl showed increasing hydrophilic properties of the permanganate hybrid by gradual loss of 14% physisorbed water up to  $100\text{ }^\circ\text{C}$  and then continued to be stable up to  $500\text{ }^\circ\text{C}$  in **Fig. 4.2b**. In this case, the parent [DSPZ].2Cl, contained almost no physisorbed water but degraded completely beyond  $300\text{ }^\circ\text{C}$  temperature.



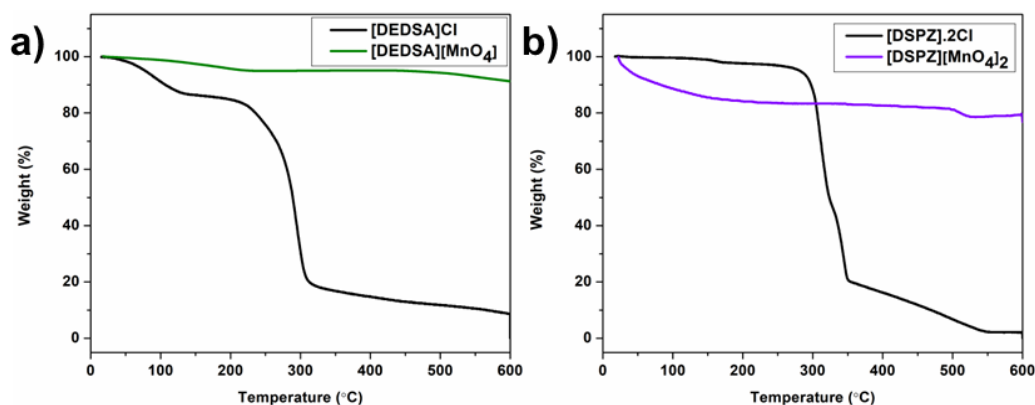


**Fig. 4.2:** Comparative Thermogravimetric analysis curve of a) [DEDSA]Cl and [DEDSA][MnO<sub>4</sub>]<sub>2</sub> b) [DSPZ].2Cl and [DSPZ][MnO<sub>4</sub>]<sub>2</sub>.

#### 4.2.1.3. Scanning Electron Microscopy (SEM) analysis

The SEM images of [DEDSA][MnO<sub>4</sub>] (**Fig. 4.3a-b**) portrayed aggregated crystalline structures of almost similar size. The morphological specification of the SEM images indicated towards the formation of agglomerates of medium scale granules, with an average size of 1.79  $\mu\text{m}$ . However, the presence of inconsistent sized granules could be seen in the SEM images of [DSPZ][MnO<sub>4</sub>]<sub>2</sub> (**Fig. 4.3d-e**). These slightly larger irregular sized granules, with an average size of 2.88  $\mu\text{m}$ , formed heterogeneous surface agglomerates. Both hybrids contained needle-like particles over the granule surfaces, which could be clearly seen in SEM images with higher resolution of the salts (**Fig. 4.3b** and **Fig. 4.3e**). Presence of intermolecular interactions within the systems could be responsible for the development of the aggregates in these salts. Formation of extensive network of H-bonding could be possible in these hybrids, owing to the polarized -SO<sub>3</sub>H groups attached to the ammonium moieties, which would significantly contribute to the heterogeneity in both the permanganate hybrids. Besides, continuous presence of oppositely charged cations and anions could also lead to the formation of ion-ion or ion-dipole interactions in the molecular arrangement, which enhanced the rigidity of the synthesized materials.

#### 4.2.1.4. Energy dispersive X-ray analysis

The Energy dispersive X-ray analysis (EDX) images of the two organic salts (**Fig. 4.3c** and **Fig. 4.3f**) depicted the presence of all the expected elements. Based on the EDX images, the existence of any unsought impurities was also ruled out.



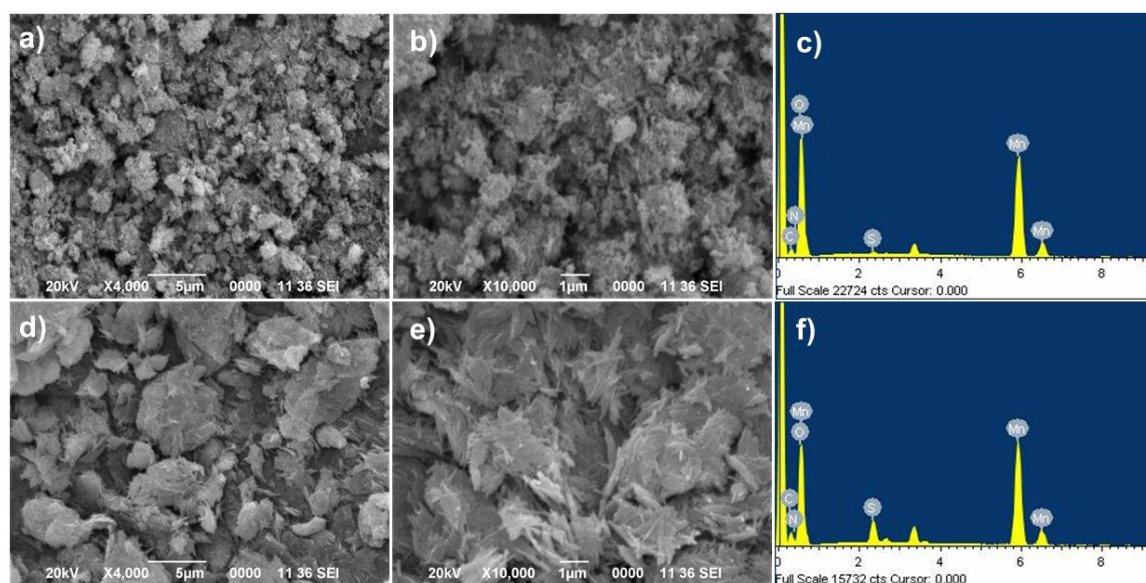


**Fig. 4.3:** a-b) SEM images of [DEDSA][MnO<sub>4</sub>], c) EDX image of [DEDSA][MnO<sub>4</sub>], d-e) SEM images of [DSPZ][MnO<sub>4</sub>]<sub>2</sub>, f) EDX image of [DSPZ][MnO<sub>4</sub>]<sub>2</sub>.

#### 4.2.1.5. Powder X-ray Diffraction pattern analysis

Powder X-ray Diffraction (PXRD) patterns of the hybrid organic salts (**Fig. 4.4**) exhibited primitive lattice configuration, as observed in case of KMnO<sub>4</sub>. However, variations in peak intensities in the XRD patterns of the hybrids were noticed after the smaller K<sup>+</sup> cation was substituted with bulkier ammonium or piperazinium cations functionalized with sulfonic acid groups. Additionally, 2θ values of the most profound KMnO<sub>4</sub> peak at 27.78°, in line with JCPDS card no. 89-3951, were found to be altered in both the [DEDSA][MnO<sub>4</sub>] and [DSPZ][MnO<sub>4</sub>]<sub>2</sub>. These changes could be the aftermath of introducing sulfonic acid functionalized organic cations to permanganate anions, as they were likely to be involved in possible inter/intra-molecular H-bonding as well as electrostatic interactions including ion-ion or ion-dipole interactions in these hybrids.

For the diethylammonium-based hybrid, 2θ values at 22.16°, 25.46°, 28.54°, 37.43°, 41.82°, 49.62°, 55.61°, 59.80°, 65.39°, 68.87° and 72.67° represented (111), (210), (211), (220), (312), (123), (214), (124), (040), (612) and (125) reflection plans, respectively. Again, for the piperazinium-based hybrid, 2θ values at 21.46°, 26.15°, 27.95°, 30.84°, 35.63°, 37.23°, 39.53°, 41.12°, 51.41°, 54.79°, 61.59° and 64.99° were designated for (111), (102), (211), (112), (121), (220), (221), (113), (230), (403), (521) and (233) reflection planes, respectively.

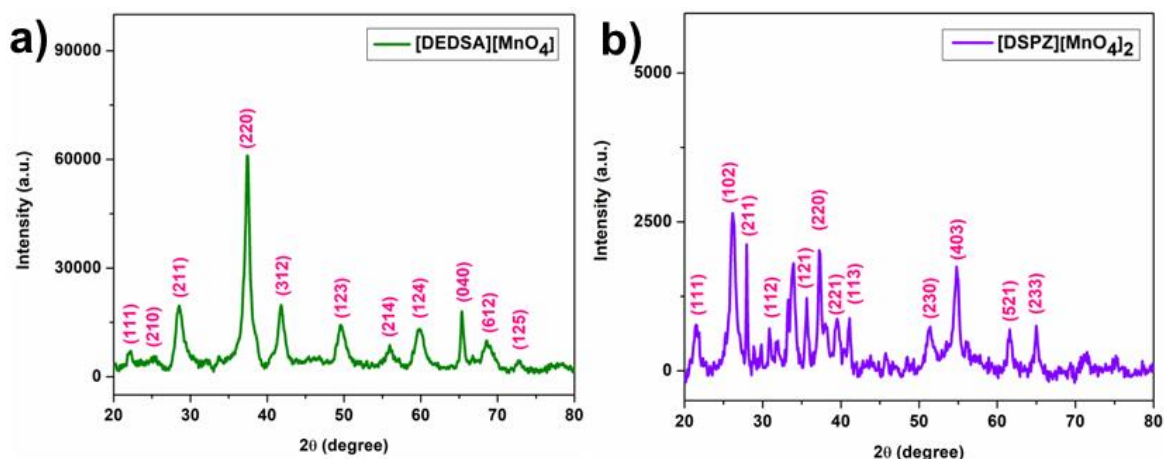


**Fig. 4.4:** PXRD pattern of a) [DEDSA][MnO<sub>4</sub>], b) [DSPZ][MnO<sub>4</sub>]<sub>2</sub>.

#### 4.2.1.6. UV-Visible Diffuse Reflectance Spectra analysis

The UV-Visible Diffuse Reflectance (DRS) spectra of both hybrids (**Fig. 4.5a-b**) were correlated with that of KMnO<sub>4</sub> (**section 4.4.5**). In case of [DEDSA][MnO<sub>4</sub>], the UV-DRS spectrum showed absorption peaks around 224 nm and 301 nm, respectively denoting  $^1A_1 \rightarrow ^1T_2$  ( $t_1 \rightarrow 4t_2$ ) and  $^1A_1 \rightarrow ^1T_2$  ( $3t_2 \rightarrow 2e$ ) electronic transitions in the permanganate anion [60]. A broad as well as very weak shoulder around 536 nm was due to  $^1A_1 \rightarrow ^1T_2$  ( $t_1 \rightarrow 2e$ ) transition in MnO<sub>4</sub><sup>-</sup> anion, whereas weak intensity peak at 371 nm could be assigned for  $^1A_1 \rightarrow ^1T_1$  ( $3t_2 \rightarrow 2e$ ) orbitally forbidden transition. Another forbidden low intensity peak for  $^1A_1 \rightarrow ^1T_1$  ( $t_1 \rightarrow 2e$ ) transition around 690 nm was undefined for both the synthesized hybrids. All these transitions also appeared in case of the permanganate hybrid of piperazinium cation with somewhat altered wavelength values. The intensities of these absorptions in the hybrids were notably reduced compared to those in KMnO<sub>4</sub>, which could be due to the diverse electronic states of MnO<sub>4</sub><sup>-</sup> anions in the synthesized materials. The reason behind this was anticipated to be the formation of strong network of H-bonding among the oxygen atoms of MnO<sub>4</sub><sup>-</sup> anion and sulfonic acid groups attached to the organic (ammonium or piperazinium) cations, which was absent in KMnO<sub>4</sub> due to the smaller size of K<sup>+</sup> cation, resulting in discrete electron transitions, contrary to the synthesized materials [61].

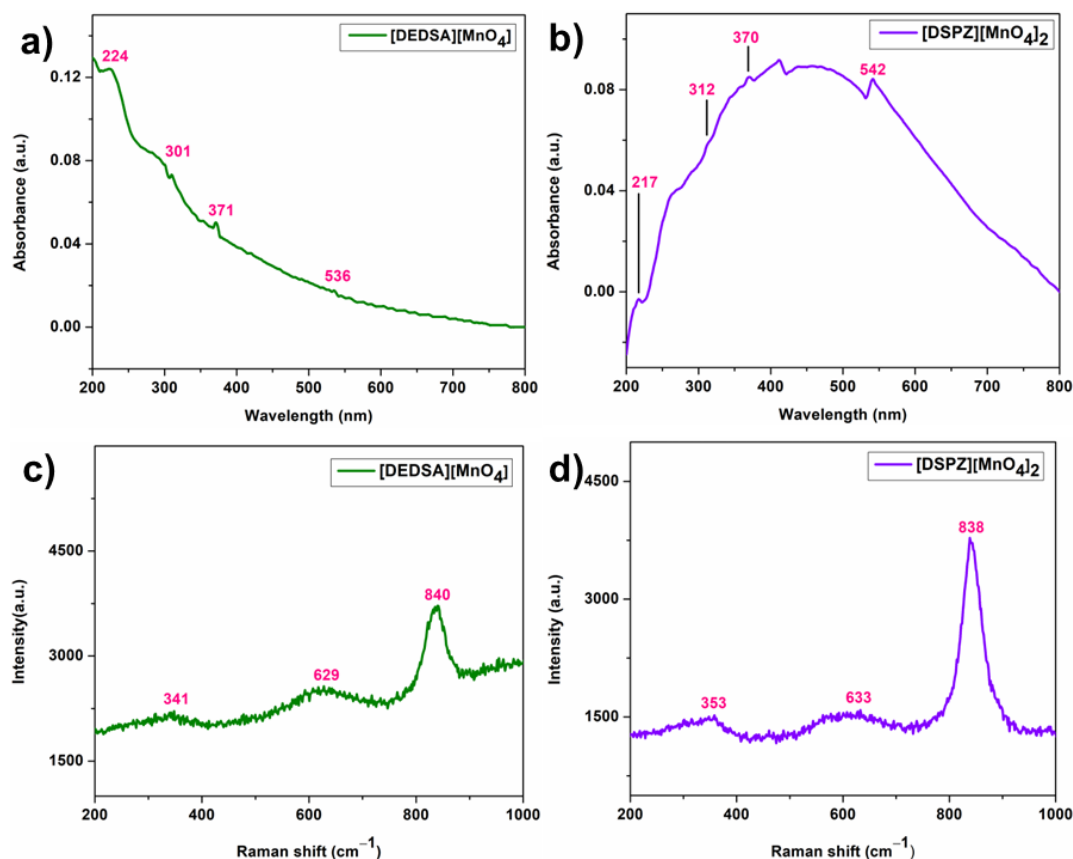


**Fig. 4.5:** UV-DRS spectra of a) [DEDSA][MnO<sub>4</sub>] and b) [DSPZ][MnO<sub>4</sub>]<sub>2</sub>; Raman spectra of c) [DEDSA][MnO<sub>4</sub>] and d) [DSPZ][MnO<sub>4</sub>]<sub>2</sub>.

#### 4.2.1.7. Raman Spectroscopy analysis

Raman spectra of both the synthesized ammonium and piperazinium-based hybrids depicted intense peaks at 840 cm<sup>-1</sup> and 838 cm<sup>-1</sup> (**Fig. 4.5c-d**), which were in accordance with the distinctive peak of MnO<sub>4</sub><sup>-</sup> anion at 840 cm<sup>-1</sup> for  $\nu_1$  ( $A_1$ ) symmetric ‘breathing’ mode (**section 4.4.5**) [62]. However, intensity of this vibration was reduced in case of [DEDSA][MnO<sub>4</sub>] peak compared to that in its piperazinium analogous as well as KMnO<sub>4</sub>. The absence of vibration for  $\nu_3$  ( $F_2$ ) mode in both the synthesized salts was blamed on the distorted tetrahedral structure of MnO<sub>4</sub><sup>-</sup> anion, which was probably caused by the formation of H-bonding along with inter/intra-ionic interactions in these hybrids as mentioned earlier. The very weakly active  $\nu_4$  ( $F_2$ ) Raman vibrations within the range of 500-400 cm<sup>-1</sup> were missing [59], contrary to their appearance in the Far-IR spectra of the hybrids (**Fig. 4.1b** and **Fig. 4.1d**). Weak vibrations for  $\nu_2$  ( $E$ ) mode of MnO<sub>4</sub><sup>-</sup> around 341 cm<sup>-1</sup> and 353 cm<sup>-1</sup> were seen for ammonium and piperazinium hybrids, respectively, like that in the precursor KMnO<sub>4</sub>. In addition, small amount of MnO<sub>2</sub> was found to be mixed

along with  $\text{MnO}_4^-$  anion in the hybrids as portrayed by the impurity peaks near  $630\text{ cm}^{-1}$  in the organic salts.

## 4.2.2. Catalytic study

### 4.2.2.1. Optimization of reaction conditions

The oxidative performances of synthesized sulfonic acid tethered ammonium-based permanganate hybrids were studied as recyclable oxidative catalysts for selective conversion of organic sulfides to sulfoxides in aqueous sulfuric acid solution as well as in aqueous solution of sulfuric acid with polar organic solvents like acetonitrile ( $\text{CH}_3\text{CN}$ ), ethyl acetate ( $\text{EtOAc}$ ) and glacial acetic acid at different temperatures. For this purpose, thioanisole (**1a**) was selected as a model organic sulfide to optimize the reaction conditions of sulfide oxidation like screening of solvents, amount of oxidative catalyst and reaction temperature. Initially, the model reaction of thioanisole (1 mmol) was conducted in acetonitrile and ethyl acetate (6 mL) under reflux temperatures using 20 mol% of the  $[\text{DEDSA}][\text{MnO}_4]$  as heterogeneous catalyst for 2 hours which did not give any product (**Table 4.1, entry 1 & 2**). Interestingly, the same amount of catalyst produced excellent yield (93%) of sulfoxide within 40 min in 10%  $\text{H}_2\text{SO}_4$  solution (6 mL) at  $80^\circ\text{C}$  in homogeneous phases (**Table 4.1, entry 3**). However, when a 1:1 mixture of acetonitrile and 10%  $\text{H}_2\text{SO}_4$  solution was used, a decent yield (79%) of desired sulfoxide product was formed (**Table 4.1, entry 4**) in 45 min of reaction time. Conducting the model reaction in biphasic 1:1 mixture of  $\text{EtOAc}$  and 10%  $\text{H}_2\text{SO}_4$  solution at  $75^\circ\text{C}$  gave only trace amount of sulfoxide in 2 hours (**Table 4.1, entry 5**). In glacial acetic acid at  $80^\circ\text{C}$ , the reaction gave sulfone as a major over-oxidized product along with minor amounts of sulfoxide and unreacted sulfide (**Table 4.1, entry 6**). While using 30 mol% of the catalyst, the increased rate of over-oxidation of sulfoxide in 10%  $\text{H}_2\text{SO}_4$  solution was noticed within 45 min reaction span (**Table 4.1, entry 7**). However, reducing the catalyst amount to 10 mol% resulted in inadequate conversion of substrate **1a** into the sulfoxide (**Table 4.1, entry 8**) in 2 hours of reaction. The yields of sulfoxide were reduced in 10%  $\text{H}_2\text{SO}_4$  solution when the reaction was performed at  $50^\circ\text{C}$  and room temperature for 2 hours (**Table 4.1, entries 9-10**). The 20 mol% of catalyst amount was also examined for the  $[\text{DSPZ}][\text{MnO}_4]_2$  hybrid in 10%  $\text{H}_2\text{SO}_4$  solution at  $80^\circ\text{C}$  which showed poor result (**Table 4.1, entry 11**). In addition,  $[\text{MDSIM}][\text{MnO}_4]$  catalyst, which could selectively convert alcohols to carbonyls as studied in **Chapter 3**, was also utilized in the oxidation of thioanisole. It was observed

that under the same reaction conditions, 20 mol% of [MDSIM][MnO<sub>4</sub>] generated impressive sulfoxide product yield (**Table 4.1, entry 11**). Thereafter, the substrate scope study for various sulfide compounds was carried out using 20 mol% of [DEDSA][MnO<sub>4</sub>] in 10% H<sub>2</sub>SO<sub>4</sub> at 80 °C temperature.

**Table 4.1:** Optimization of model reaction for sulfide oxidation using [DEDSA][MnO<sub>4</sub>] hybrid catalyst.

Entry	Catalyst	Catalyst amount (mol%)	Solvent	Temp (°C)	Time (min) <sup>[a]</sup>	pH	%Yield <sup>[b]</sup> ( <b>2a</b> )
1	[DEDSA][MnO <sub>4</sub> ]	20	CH <sub>3</sub> CN	80	120	-	-
2	[DEDSA][MnO <sub>4</sub> ]	20	EtOAc	80	120	-	-
<b>3</b>	<b>[DEDSA][MnO<sub>4</sub>]</b>	<b>20</b>	<b>10% H<sub>2</sub>SO<sub>4</sub></b>	<b>80</b>	<b>40</b>	<b>1</b>	<b>93</b>
4	[DEDSA][MnO <sub>4</sub> ]	20	CH <sub>3</sub> CN + 10% H <sub>2</sub> SO <sub>4</sub>	80	45	1	79
5	[DEDSA][MnO <sub>4</sub> ]	20	EtOAc + 10% H <sub>2</sub> SO <sub>4</sub>	75	120	1	Trace
6	[DEDSA][MnO <sub>4</sub> ]	20	Glacial acetic acid	80	120	3	22 <sup>[c]</sup>
7	[DEDSA][MnO <sub>4</sub> ]	30	10% H <sub>2</sub> SO <sub>4</sub>	80	45	1	80
8	[DEDSA][MnO <sub>4</sub> ]	10	10% H <sub>2</sub> SO <sub>4</sub>	80	120	1	61
9	[DEDSA][MnO <sub>4</sub> ]	20	10% H <sub>2</sub> SO <sub>4</sub>	50	120	1	79
10	[DEDSA][MnO <sub>4</sub> ]	20	10% H <sub>2</sub> SO <sub>4</sub>	R.T.	120	1	67
11	[DSPZ][MnO <sub>4</sub> ] <sub>2</sub>	20	10% H <sub>2</sub> SO <sub>4</sub>	80	45	1	38
12	[MDSIM][MnO <sub>4</sub> ]	20	10% H <sub>2</sub> SO <sub>4</sub>	80	45	1	90 <sup>[d]</sup>

<sup>[a]</sup> Using 1 mmol of thioanisole as model substrate. <sup>[b]</sup> Isolated yield. <sup>[c]</sup> Major product sulfone (61% yield). <sup>[d]</sup> %Yield of sulfoxide obtained by using [MDSIM][MnO<sub>4</sub>], which was studied in **Chapter 3**.

#### 4.2.2.2. Substrate scope study

The substrate scope study for the selective oxidation of sulfides under the optimized conditions (**Fig. 4.6**) showed that sulfides such as thioanisole, diphenyl sulfide and benzyl phenyl sulfide produced an excellent yield of corresponding sulfoxide products (>90%) within an hour of reaction time. Dibenzothiophene also generated satisfactory

product yield in a relatively longer reaction span. In the case of allyl phenyl sulfide, formation of allyl phenyl sulfoxide with a 77% yield showed the chemoselective nature of the catalyst. However, the presence of small amount of dihydroxylated product was also detected along with the major sulfoxide product. Regarding the substituted thioanisoles, 4-nitrothioanisole and 4-bromothioanisole produced reasonable yields of sulfoxides, but 4-(methylthio)aniline showed no reaction up to 2 hours of reaction time. Spectral data and the spectra of the sulfoxide products are given in section 4.4.6, 4.4.7, 4.4.8.

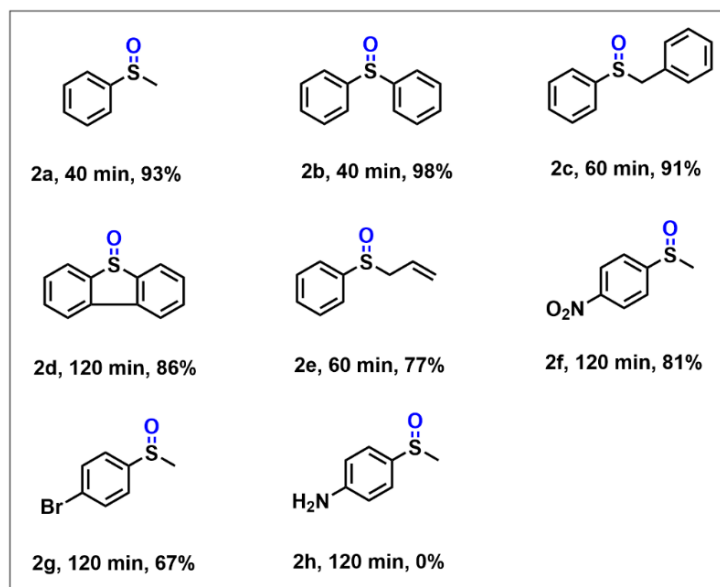


**Fig. 4.6:** Oxidation of organic sulfides under the optimized conditions using 20 mol% of [DEDSA][MnO<sub>4</sub>] catalyst.

A comparative study was performed between the present work and earlier reports, as shown in **Table 4.2**, which showed the better sustainability of this catalytic system in an aqueous solution of sulfuric acid without the use of any external oxidants for controlled oxidation of the sulfide, where sulfuric acid acted as a co-catalyst according to the proposed mechanism.

**Table 4.2:** A comparison of the model reaction in the present work with earlier reports of sulfide oxidation.

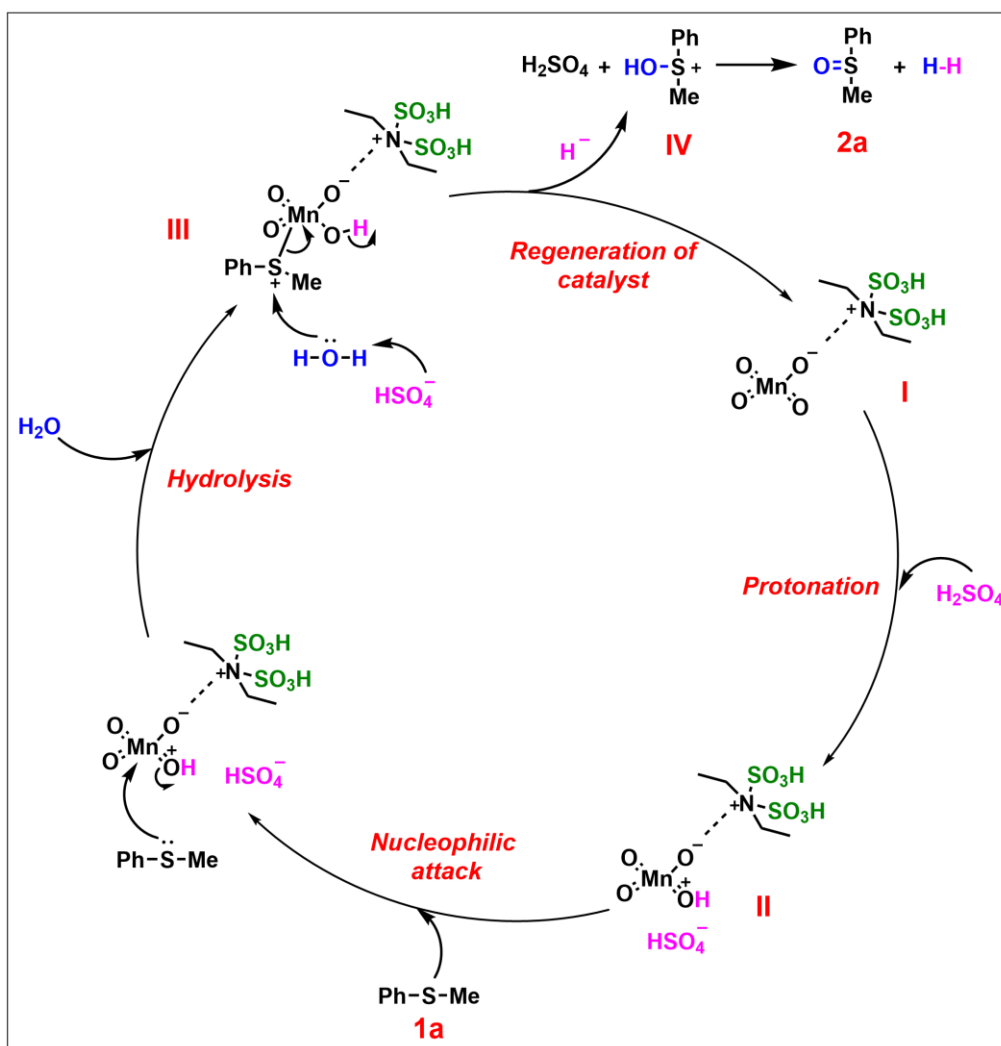
Entry	Solvent	Catalyst	Oxidant	Temp (°C)	Time	%Yields [Ref.]
1	[Bmim][BF <sub>4</sub> ]	-	H <sub>2</sub> O <sub>2</sub> (20 mmol)	25	4 h	95 [22]

2	H <sub>2</sub> O	Mn(OAc) <sub>2</sub> / [C <sub>12</sub> mim][NO <sub>3</sub> ] (0.2 mol/20 mL)	Molecular oxygen (50 mL min <sup>-1</sup> )	50	2 h	97 [63]
3	-	[Hmim]HSO <sub>4</sub> (2 mmol)	Ceric ammonium nitrate (CAN) (1 mmol)	80	5 min	94 [64]
4	CH <sub>3</sub> CN	VO <sub>2</sub> F(dmpz) <sub>2</sub> (0.02 mmol)	H <sub>2</sub> O <sub>2</sub> (2.2 mmol)	0-5	5 h	95 [65]
5	2,2,2- Trifluoroethanol (TFE)	Fe(NO <sub>3</sub> ) <sub>3</sub> ·9H <sub>2</sub> O (5 mol%)	O <sub>2</sub> (0.2 MPa)	80	4 h	95 [66]
6	CH <sub>3</sub> CN	Ru(PVP)/γ-Al <sub>2</sub> O <sub>3</sub> (0.5 mmol)	H <sub>2</sub> O <sub>2</sub> (1 mmol)	R.T.	120 min	98 [67]
7	10% H <sub>2</sub> SO <sub>4</sub>	[DEDSA][MnO <sub>4</sub> ] (20 mol%)	-	80	40 min	93 [This work]

#### 4.2.2.3. Plausible mechanism

The plausible mechanism of sulfide oxidation catalyzed by [DEDSA][MnO<sub>4</sub>] hybrid could be illustrated in **Scheme 4.3** for the model substrate (**1a**) in acidic solution. In an acidic environment, the permanganate anion of the hybrid catalyst **I** undergoes protonation and thereby acts as an electron-deficient metal center in intermediate **II** along with HSO<sub>4</sub><sup>-</sup> as a counter anion. Then, nucleophilic attack by thioanisole (**1a**) to the metal center of permanganate anion of intermediate **II** occurs and leads to formation of intermediate **III**. Thereafter, the HSO<sub>4</sub><sup>-</sup> initiated proton abstraction and hydrolysis of intermediate **III** could be expected, involving nucleophilic attack by a water molecule of the electrophilic S atom of intermediate **III**, followed by cleavage of Mn-S bond along with elimination of a H<sup>-</sup> anion as a hydrogen molecule in acidic solution, which regenerates the permanganate hybrid **I**. Finally, the sulfonium intermediate **IV** yields the sulfoxide product after releasing the acidic proton to the reaction medium.





**Scheme 4.3:** Plausible mechanism for the oxidation of sulfides to sulfoxides with [DEDSA][MnO<sub>4</sub>] salt.

#### 4.2.3. Catalyst recyclability

The recyclability of [DEDSA][MnO<sub>4</sub>] oxidative catalyst was examined for 3 mmol scale of the model substrate after successful execution of the 1<sup>st</sup> reaction under the optimized reaction conditions. To recover the used catalyst from aqueous 10% H<sub>2</sub>SO<sub>4</sub> layer after extraction of product sulfoxide in organic extract, as mentioned in experimental procedure, 10% NaOH solution was added dropwise to neutralize the aqueous acidic solution for complete precipitation of the permanganate hybrid in one hour. The precipitate was then collected by centrifugation and washed with distilled water (× 3 times) as well as acetone (× 2 times). After drying it under vacuum for 24 h, the recovered catalyst was obtained which was further analyzed using FT-IR, PXRD and EDX to check its integrity before subjecting it to another cycle of reaction. The catalyst could be used up to four

consecutive cycles of reaction, although a significant decrease in product yield at comparable reaction time was observed after each cycle (**Fig. 4.7a**). The reason behind this could be the probable loss of catalyst activity, owing to its repeated washing and drying in vacuum after each cycle. The PXRD pattern of the recovered catalyst after the 4th cycle of reaction displayed shifting of peaks as compared to that of fresh catalyst, along with appearance of additional diffractions (**Fig. 4.7b**). The FT-IR spectrum of the recovered catalyst showed retention of most absorbances exhibited by the fresh catalyst with slightly varied intensities (**Fig. 4.7c**). These variations shown by the recovered catalyst could be linked to its repeated treatment with aqueous NaOH solution for neutralization and then reactivation after each cycle, leading to a subtle distortion in the catalyst structure. The EDX image depicted the presence of all the relevant elements in the recovered catalyst (**Fig. 4.7d**).

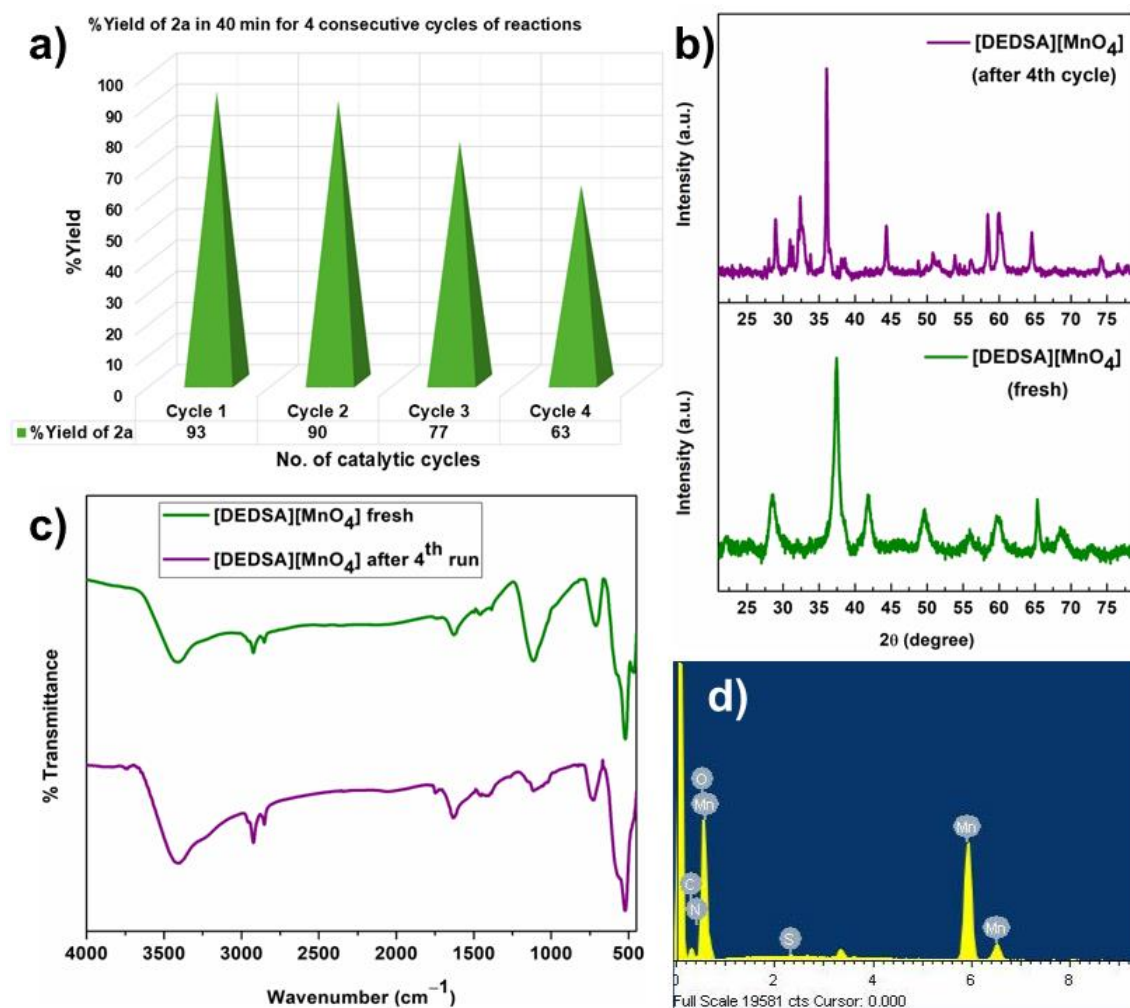


**Fig. 4.7:** a) Bar diagram of catalyst recyclability, b) PXRD of reused catalyst, c) FT-IR of reused catalyst, d) EDX image of recovered catalyst.

### 4.3. Summary

Briefly, two organic-inorganic hybrids of sulfonic acid functionalized ammonium and piperazinium-based cations with permanganate anion were developed as sustainable oxidants by anion-exchange reactions of  $\text{KMnO}_4$  with the respective precursor of chloride-based ammonium salts. Structural compositions and thermal stabilities of both hybrids were studied using FT-IR, SEM, EDX, UV-Vis DRS, PXRD, Raman and TGA techniques, respectively. Oxidative power of these hybrids was examined as efficient internal oxidative catalysts for selective oxidation of sulfides to sulfoxides in 10% aqueous sulfuric acid solution at 80 °C. where sulfuric acid acted as co-catalyst. The catalyst was also found to be recyclable up to 4 cycles of sulfide oxidation reactions.

### 4.4. Experimental section

#### 4.4.1. Synthesis of N, N'-diethyldisulfoammonium permanganate ( $[\text{DEDSA}][\text{MnO}_4]$ ) and 1,4-disulfopiperazinium permanganate ( $[\text{DSPZ}][\text{MnO}_4]_2$ ) hybrids

N, N'-diethyldisulfoammonium permanganate ( $[\text{DEDSA}][\text{MnO}_4]$ ) hybrid was prepared *via* formation of precursor N, N'-diethyldisulfoammonium chloride ( $[\text{DEDSA}]\text{Cl}$ ) ionic liquid which was subjected to anion-exchange reaction with  $\text{KMnO}_4$  (**Scheme 4.1**). Firstly, 10 mmol of diethylamine in 30 mL dry hexane was dealt with 20 mmol of chlorosulfonic acid at room temperature for 1 h, as per the standard procedure, to get 96% yield of the  $[\text{DEDSA}]\text{Cl}$  as brown viscous liquid [57]. 9 mmol of the resultant  $[\text{DEDSA}]\text{Cl}$  ionic liquid was then added dropwise to 9 mmol of aqueous  $\text{KMnO}_4$  (in 30 mL distilled water) solution with continuous stirring at room temperature for the exchange reaction of chloride anion with permanganate anion to occur. The reaction was stirred for 3 h and the brownish black precipitate of permanganate hybrid of ammonium cation was collected by centrifugation, washed thoroughly with distilled water and dried under vacuum at 80 °C for 24 h to obtain 95% yield of  $[\text{DEDSA}][\text{MnO}_4]$  hybrid.

Similarly, the anion-exchange reaction of 1,4-disulfopiperazinium chloride ( $[\text{DSPZ}].2\text{Cl}$ ) salt with permanganate anion was carried out with aqueous solution of  $\text{KMnO}_4$  to get 1,4-disulfopiperazinium permanganate hybrid ( $[\text{DSPZ}][\text{MnO}_4]_2$ ) (**Scheme 4.1**). To start this process, 20 mmol of chlorosulfonic acid was added dropwise to a solution of 10 mmol of piperazine in dry  $\text{CH}_2\text{Cl}_2$  in a 100 mL round bottom flask at room temperature, according to reported literature, which produced 95% yield of  $[\text{DSPZ}].2\text{Cl}$

ionic salt as a white solid after stirring for 1 h [58]. The exchange of chloride anion of this organic salt with permanganate anion took place when 9 mmol of [DSPZ].2Cl was reacted with 18 mmol of aqueous  $\text{KMnO}_4$  solution at room temperature for 3 h. The reaction mixture was centrifuged, washed thoroughly with distilled water. After drying the precipitate at 80 °C in a vacuum oven, the brownish black precipitate was collected as 94% yield of [DSPZ][ $\text{MnO}_4$ ]<sub>2</sub> hybrid.

#### 4.4.2. Typical method for oxidation of organic sulfides to sulfoxides using [DEDSA][ $\text{MnO}_4$ ] as catalyst

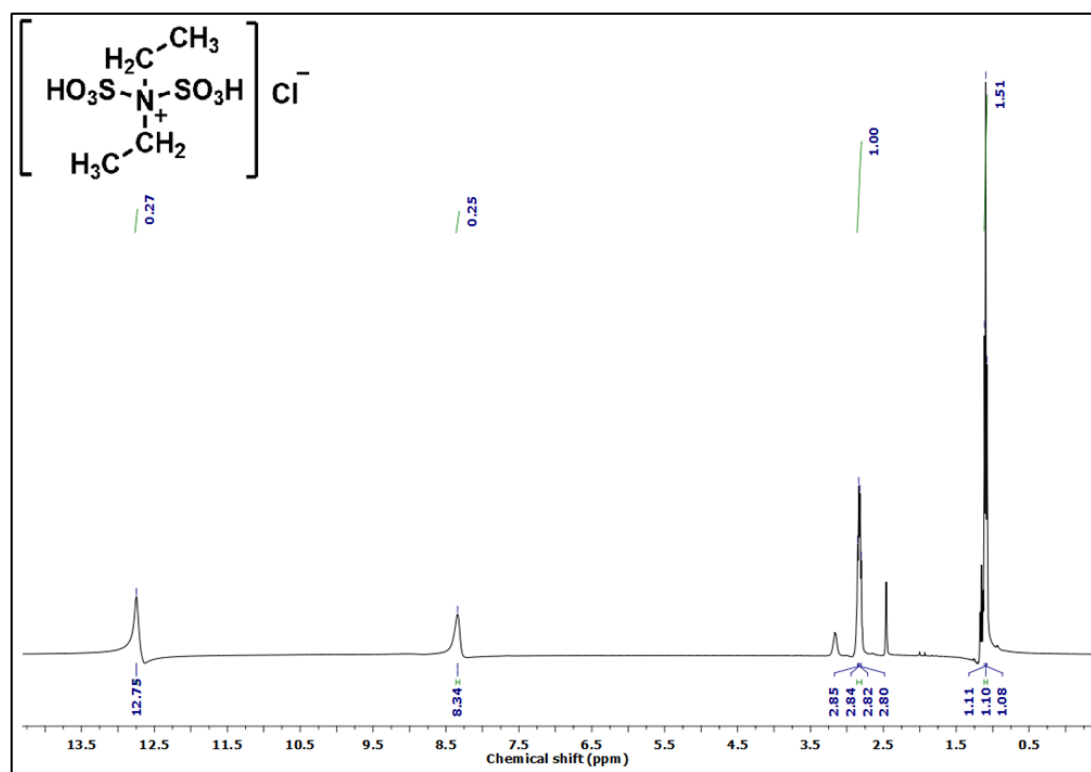
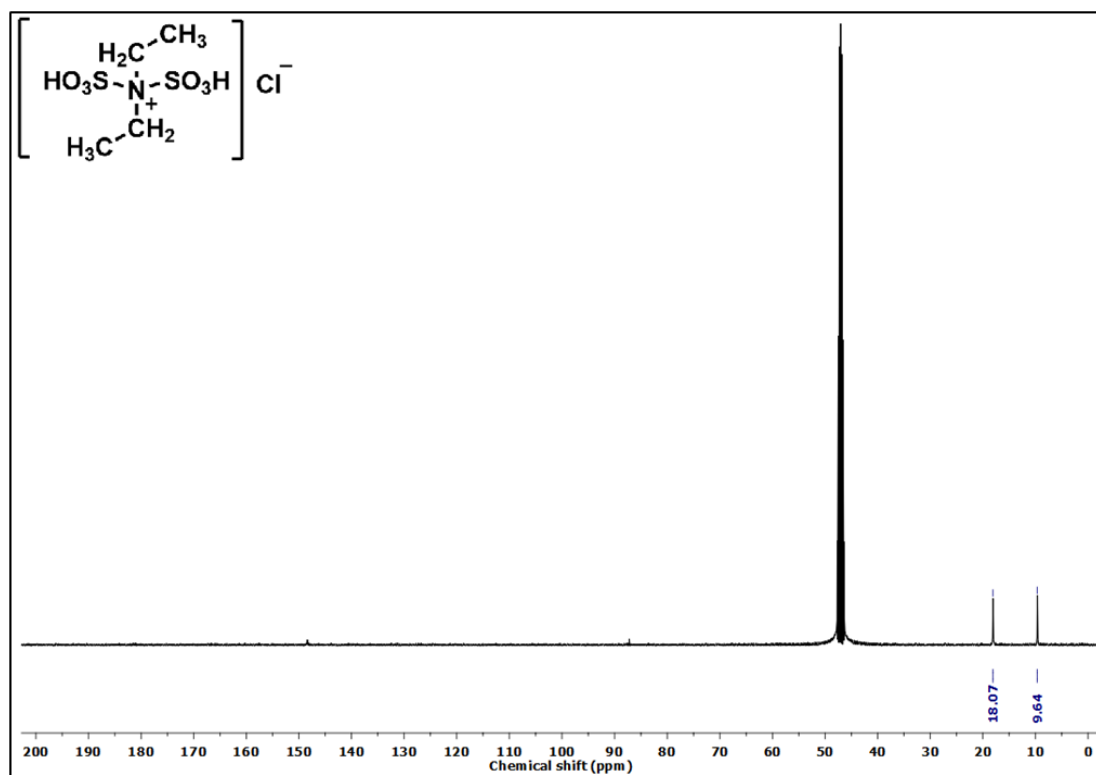
For oxidation of sulfides to sulfoxides, 1 mmol of the organic sulfide compound was taken in a 100 mL two-necked round bottom flask containing 6 mL of 10% aqueous sulfuric acid solution (**Scheme 4.2**). Then the reaction mixture was stirred at 80 °C under reflux condition for the specified reaction time after the addition of 20 mol% of [DEDSA][ $\text{MnO}_4$ ] catalyst till the reaction was completed as monitored by thin layer chromatographic technique (TLC). After that, the product was extracted from acidic aqueous solution with dichloromethane ( $3 \times 5$  mL) and dried over anhydrous sodium sulfate. Evaporation of the dichloromethane extract under reduced pressure produced the crude product of sulfoxide for GC-MS analysis. The yield% of sulfoxide was attained after purification of crude product using column chromatography. Subsequently, the used permanganate catalyst was recovered from the acidic aqueous layer through precipitation after neutralization with 10% aqueous NaOH solution, which then filtered, washed with distilled water and dried in vacuum oven at 80 °C for reactivation.

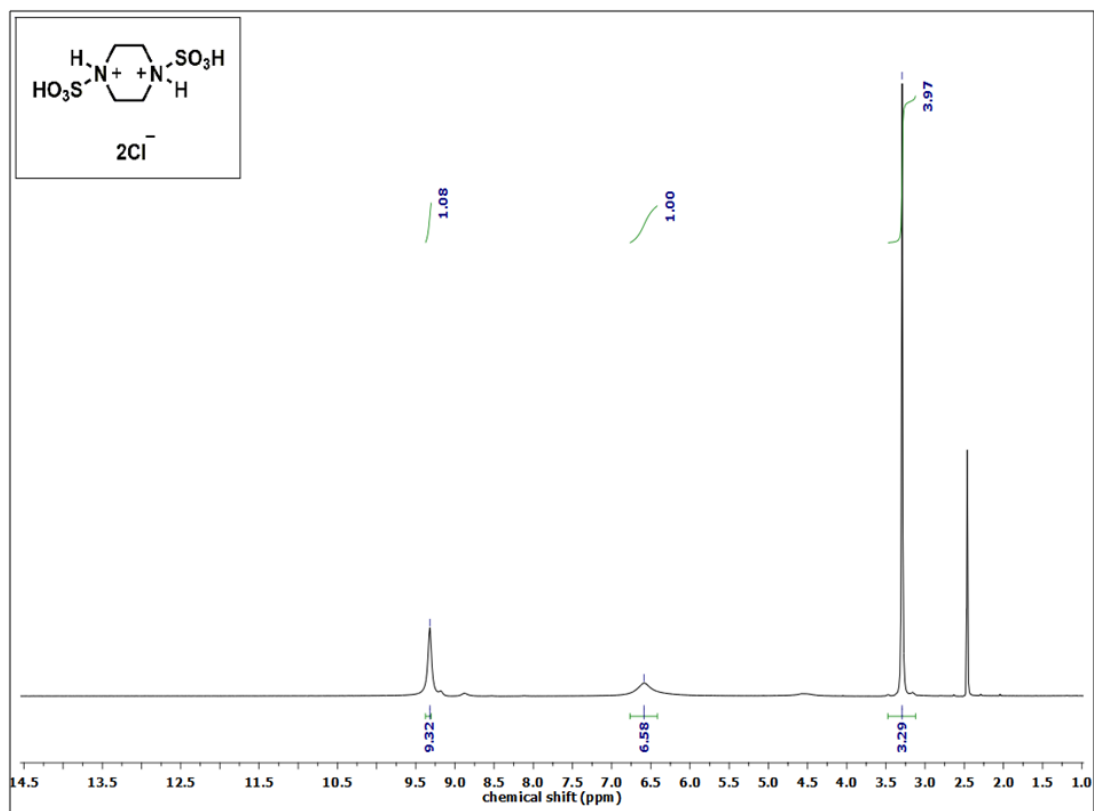
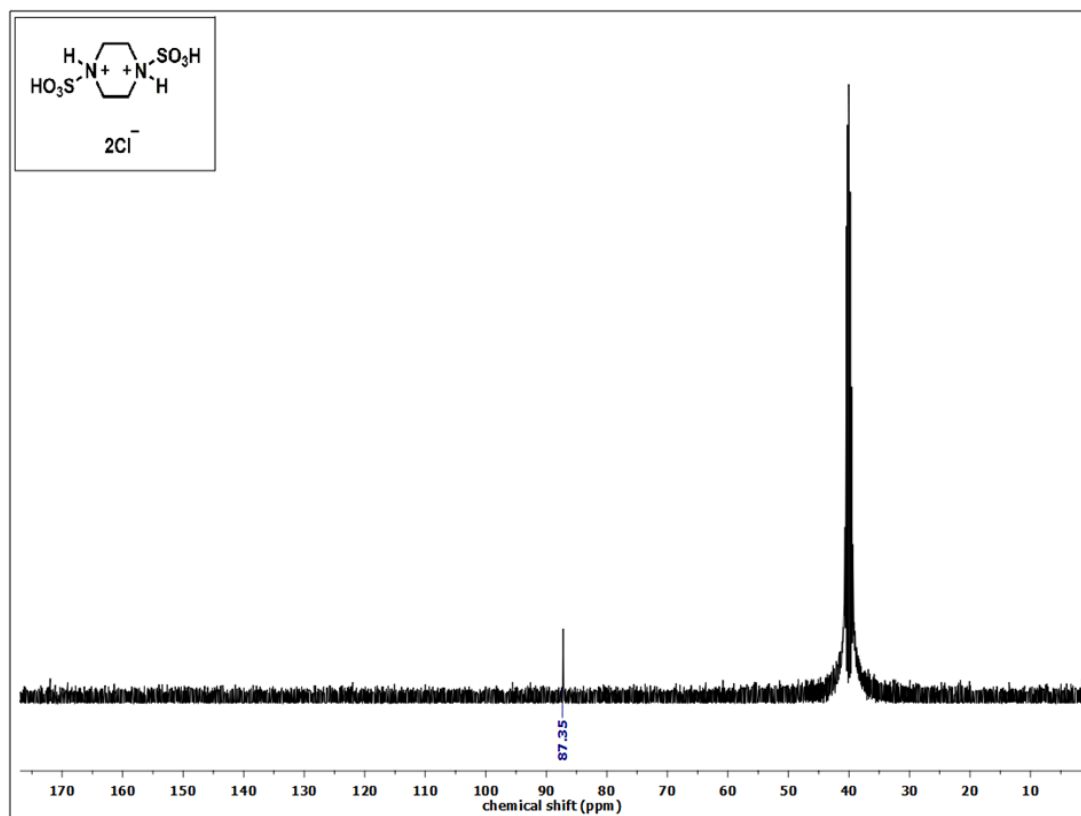
#### 4.4.3. Spectral data of parent organic salts

[DEDSA]Cl: Yellowish brown liquid,  $^1\text{H}$  NMR ( $\text{CDCl}_3$ , 400 MHz):  $\delta$  12.75 (s, 1 H), 8.34 (s, 1 H), 2.83 (q,  $J = 8.0$  Hz, 4 H), 1.10 (t,  $J = 8.0$  Hz, 6 H);  $^{13}\text{C}$  NMR ( $\text{CDCl}_3$ , 100 MHz):  $\delta$  18.07, 9.64.

[DSPZ].2Cl: White solid,  $^1\text{H}$  NMR ( $\text{DMSO}-d_6$ , 400 MHz):  $\delta$  9.32 (s, 2H), 6.58 (s, 2H), 3.29 (s, 8H);  $^{13}\text{C}$  NMR ( $\text{DMSO}-d_6$ , 100 MHz):  $\delta$  87.35.

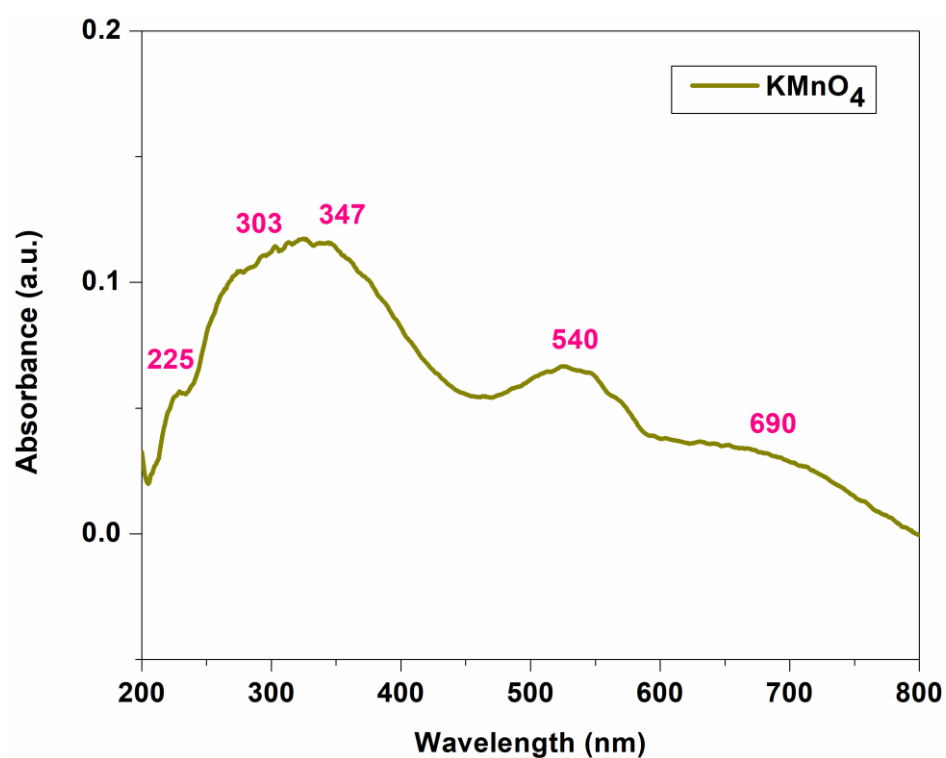
## 4.4.4. NMR spectra of parent organic salts

a)  $^1\text{H}$  NMR of  $[\text{DEDSA}]\text{Cl}$ b)  $^{13}\text{C}$  NMR of  $[\text{DEDSA}]\text{Cl}$ 

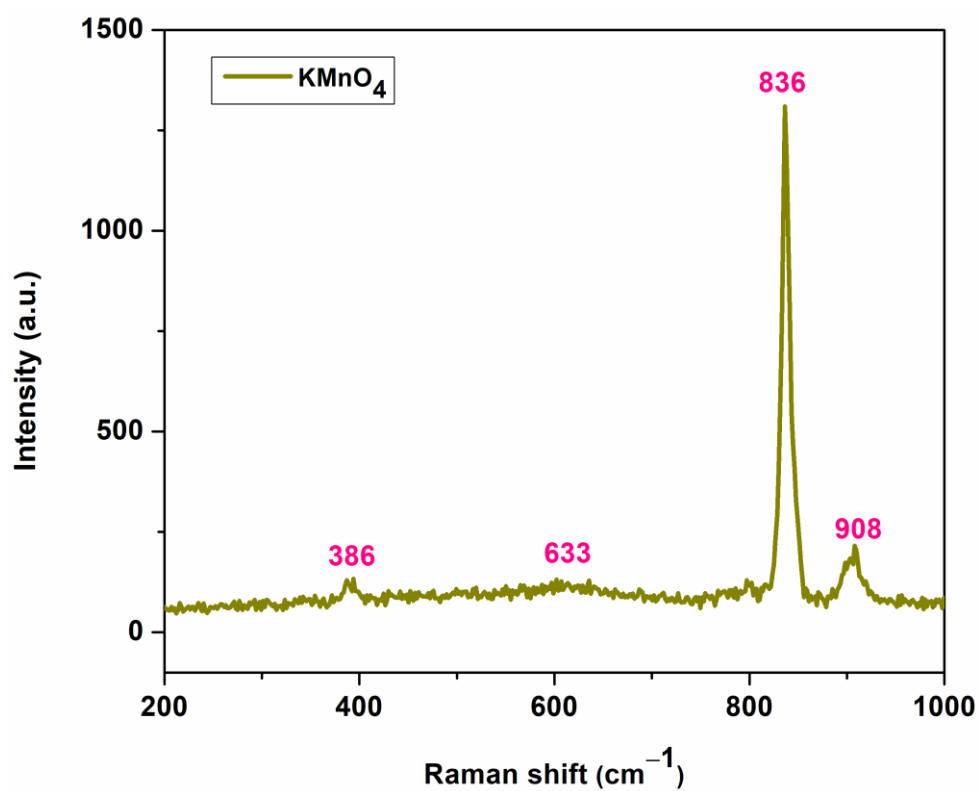
c)  $^1\text{H}$  NMR of  $[\text{DSPZ}].2\text{Cl}$ d)  $^{13}\text{C}$  NMR of  $[\text{DSPZ}].2\text{Cl}$ 

#### 4.4.5. Spectra of solid potassium permanganate ( $\text{KMnO}_4$ )

a) UV-Vis DRS spectrum of  $\text{KMnO}_4$

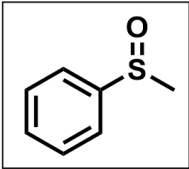
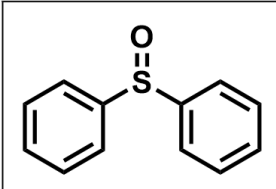
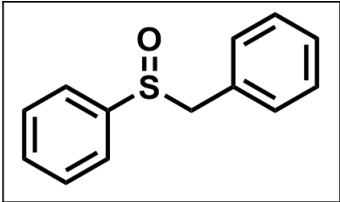
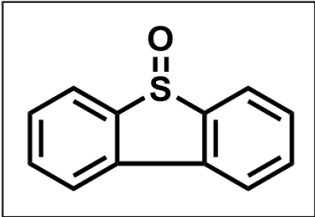


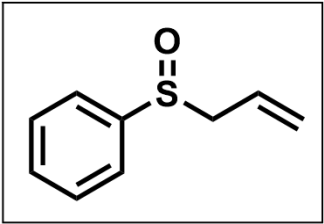
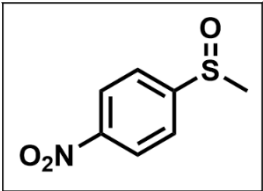
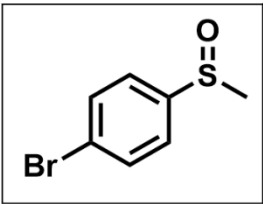
b) Raman spectrum of  $\text{KMnO}_4$



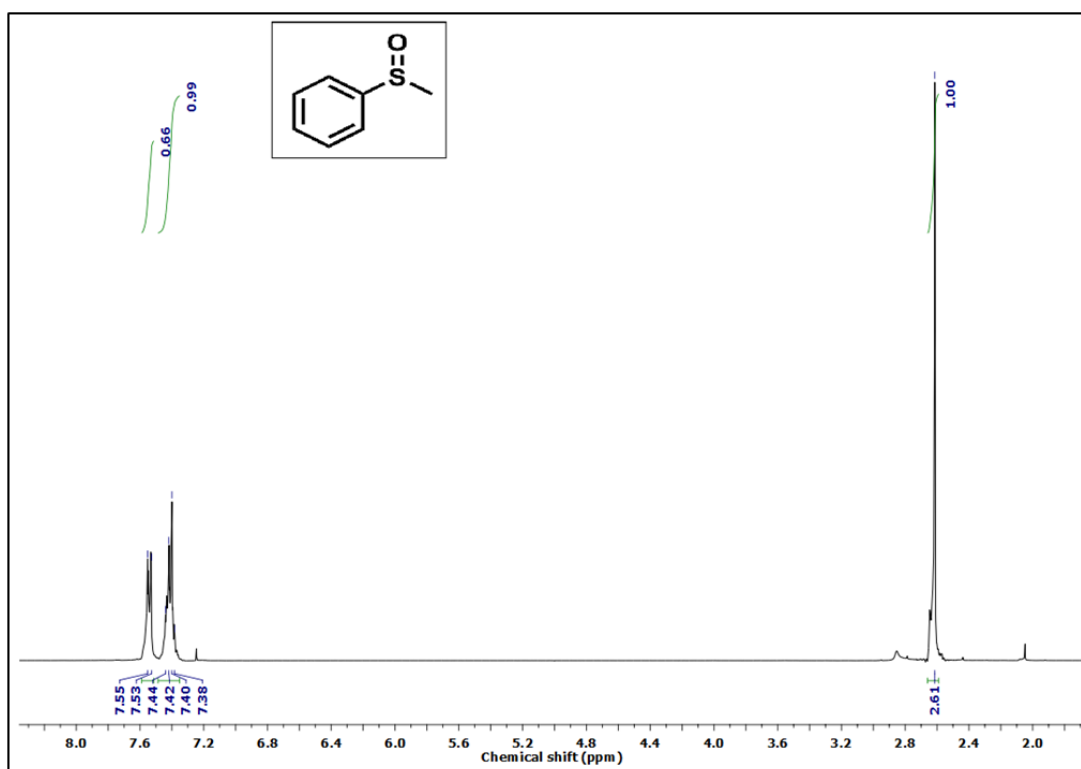
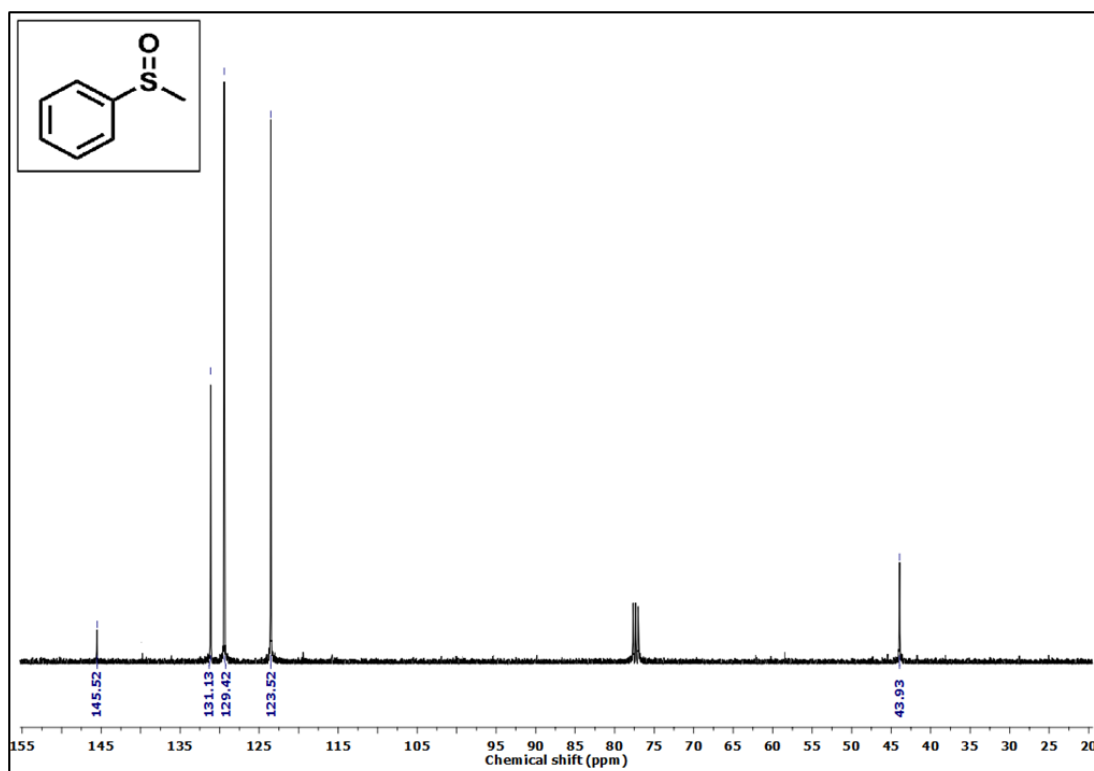


## 4.4.6. Spectral data of sulfoxide products

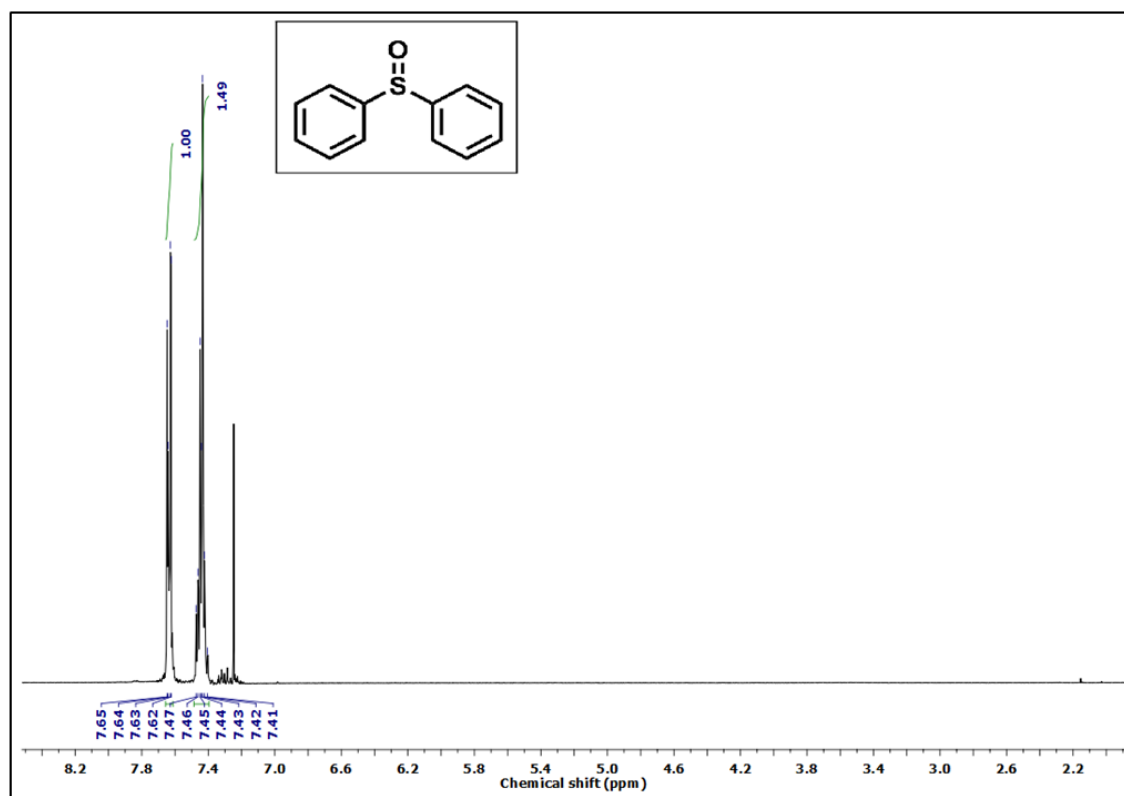
Product name	Spectral data
 <p>Methyl phenyl sulfoxide (<b>2a</b>)</p>	<p>White solid, Mp. 32 °C, <math>^1\text{H}</math> NMR (<math>\text{CDCl}_3</math>, 400 MHz): <math>\delta</math> 7.55-7.53 (m, 2H), 7.44-7.38 (m, 3H), 2.61 (s, 3H); <math>^{13}\text{C}</math> NMR (<math>\text{CDCl}_3</math>, 100 MHz): <math>\delta</math> 145.42, 131.13, 129.42, 123.52, 43.93; GC-MS <math>m/z</math> values 140 (<math>\text{M}^+</math>), 125, 109, 98, 77, 63, 51 (100%).</p>
 <p>Diphenyl sulfoxide (<b>2b</b>)</p>	<p>White solid, Mp. 70 °C, <math>^1\text{H}</math> NMR (<math>\text{CDCl}_3</math>, 400 MHz): <math>\delta</math> 7.65-7.62 (m, 4H), 7.47-7.41 (m, 6H); <math>^{13}\text{C}</math> NMR (<math>\text{CDCl}_3</math>, 100 MHz): <math>\delta</math> 131.15, 129.44, 124.89; GC-MS <math>m/z</math> values 202 (<math>\text{M}^+</math>, 100%), 186, 154, 125, 109, 77, 51.</p>
 <p>Benzyl phenyl sulfoxide (<b>2c</b>)</p>	<p>White solid, Mp. 123 °C, <math>^1\text{H}</math> NMR (<math>\text{CDCl}_3</math>, 400 MHz): <math>\delta</math> 7.45-7.35 (m, 5H), 7.28-7.21 (m, 3H), 6.98 (d, <math>J</math> = 8.0 Hz, 2H), 4.10-3.97 (dd, <math>J</math> = 12 Hz, 40 Hz, 2H); <math>^{13}\text{C}</math> NMR (<math>\text{CDCl}_3</math>, 100 MHz): <math>\delta</math> 142.81, 131.26, 130.44, 129.19, 128.94, 128.54, 128.34, 124.53, 58.38.</p>
 <p>Dibenzothiophene-5-oxide (<b>2d</b>)</p>	<p>White solid, Mp. 188 °C, <math>^1\text{H}</math> NMR (<math>\text{CDCl}_3</math>, 400 MHz): <math>\delta</math> 7.99 (d, <math>J</math> = 8.0 Hz, 2H), 7.82-7.80 (d, <math>J</math> = 8.0 Hz, 2H), 7.59 (t, <math>J</math> = 8.0 Hz, 2H), 7.50 (t, <math>J</math> = 8.0 Hz, 2H); <math>^{13}\text{C}</math> NMR (<math>\text{CDCl}_3</math>, 100 MHz): <math>\delta</math> 137.77, 134.00, 131.70, 130.49, 122.29, 121.68; GC-MS: <math>m/z</math> 201 (<math>\text{M}+1^+</math>), 185 (100%), 170, 140, 124, 108, 96, 76, 63, 51.</p>

 <p>Allyl phenyl sulfoxide (<b>2e</b>)</p>	<p>Brownish liquid, <math>^1\text{H}</math> NMR (<math>\text{CDCl}_3</math>, 400 MHz): <math>\delta</math> 7.86-7.84 (m, 2H), 7.65-7.51 (m, 3H), 5.82-5.72 (m, 1H), 5.30 (t, <math>J = 8.0</math> Hz, 1H), 5.15-5.10 (dd, <math>J = 4</math> Hz, 16 Hz, 1H), 3.80 (d, <math>J = 8.0</math> Hz, 2H); <math>^{13}\text{C}</math> NMR (<math>\text{CDCl}_3</math>, 100 MHz): <math>\delta</math> 138.28, 133.88, 129.16, 128.57, 124.88, 124.67, 60.94.</p>
 <p>Methyl 4-nitrophenyl sulfoxide (<b>2f</b>)</p>	<p>Off white solid, Mp. 148 °C, <math>^1\text{H}</math> NMR (<math>\text{CDCl}_3</math>, 400 MHz): <math>\delta</math> 8.39-8.37 (d, <math>J = 8.0</math> Hz, 2H), 7.83-7.81 (d, <math>J = 8.0</math> Hz, 2H), 2.78 (s, 3H); <math>^{13}\text{C}</math> NMR (<math>\text{CDCl}_3</math>, 100 MHz): <math>\delta</math> 153.27, 149.58, 124.75, 124.59, 43.94; GC-MS <math>m/z</math> values 185 (<math>\text{M}^+</math>), 184 (100%), 171, 158, 152, 139, 138, 113, 98, 91, 79, 63, 51.</p>
 <p>Methyl 4-bromophenyl sulfoxide (<b>2g</b>)</p>	<p>Off white solid, Mp. 86 °C, <math>^1\text{H}</math> NMR (<math>\text{CDCl}_3</math>, 400 MHz): <math>\delta</math> 7.66-7.64 (d, <math>J = 8.0</math> Hz, 2H), 7.51-7.49 (d, <math>J = 8.0</math> Hz, 2H), 2.70 (s, 3H); <math>^{13}\text{C}</math> NMR (<math>\text{CDCl}_3</math>, 100 MHz): <math>\delta</math> 144.86, 132.68, 125.57, 125.23, 44.06; GC-MS <math>m/z</math> values 220 (<math>\text{M}^+</math>), 218 (<math>\text{M}^+</math>), 189, 187, 157, 155, 131, 129, 108, 91, 89, 81, 79, 76, 63, 51.</p>

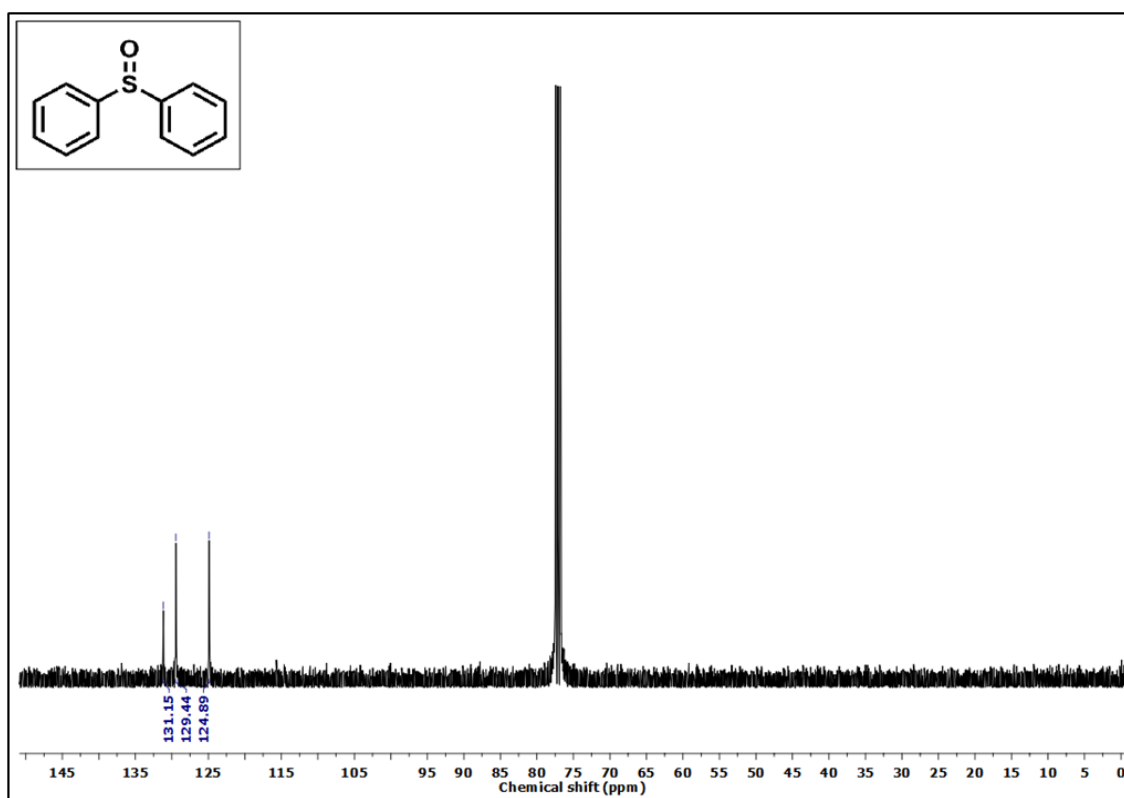
## 4.4.7. NMR spectra of sulfoxide products

a)  $^1\text{H}$  NMR of methyl phenyl sulfoxide (**2a**)b)  $^{13}\text{C}$  NMR of methyl phenyl sulfoxide (**2a**)

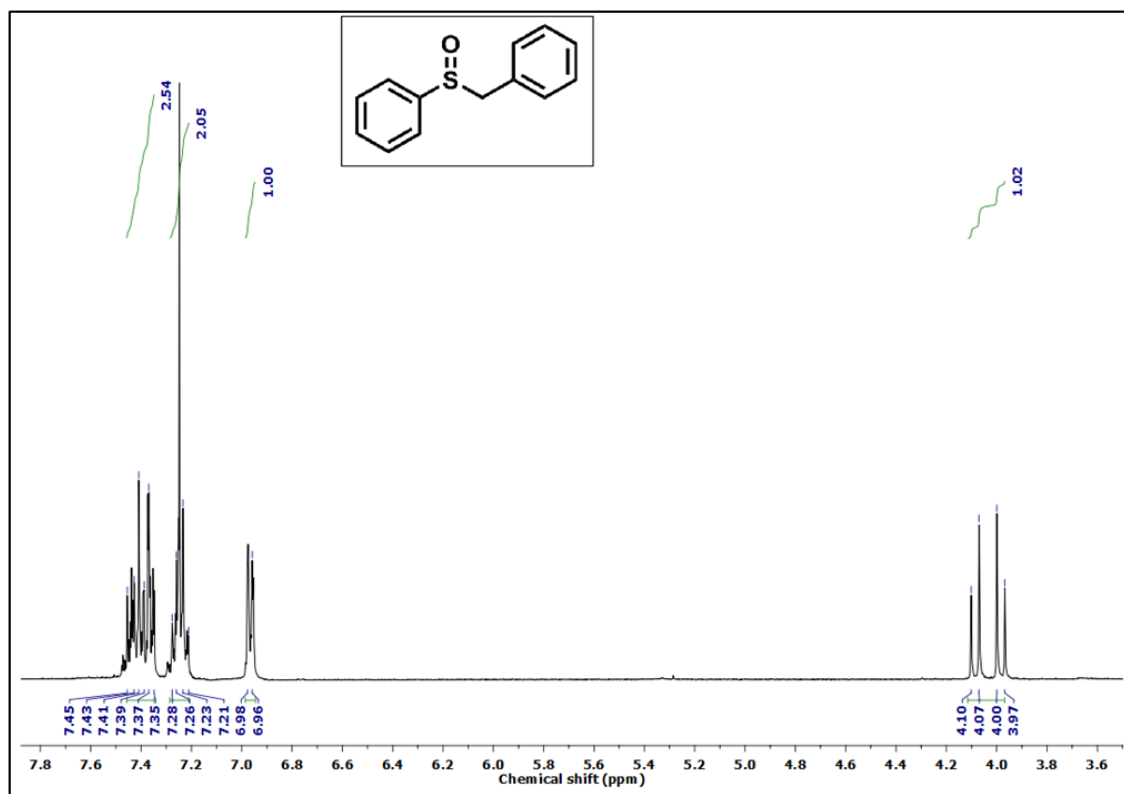
c)  $^1\text{H}$  NMR spectrum of diphenyl sulfoxide (**2b**)



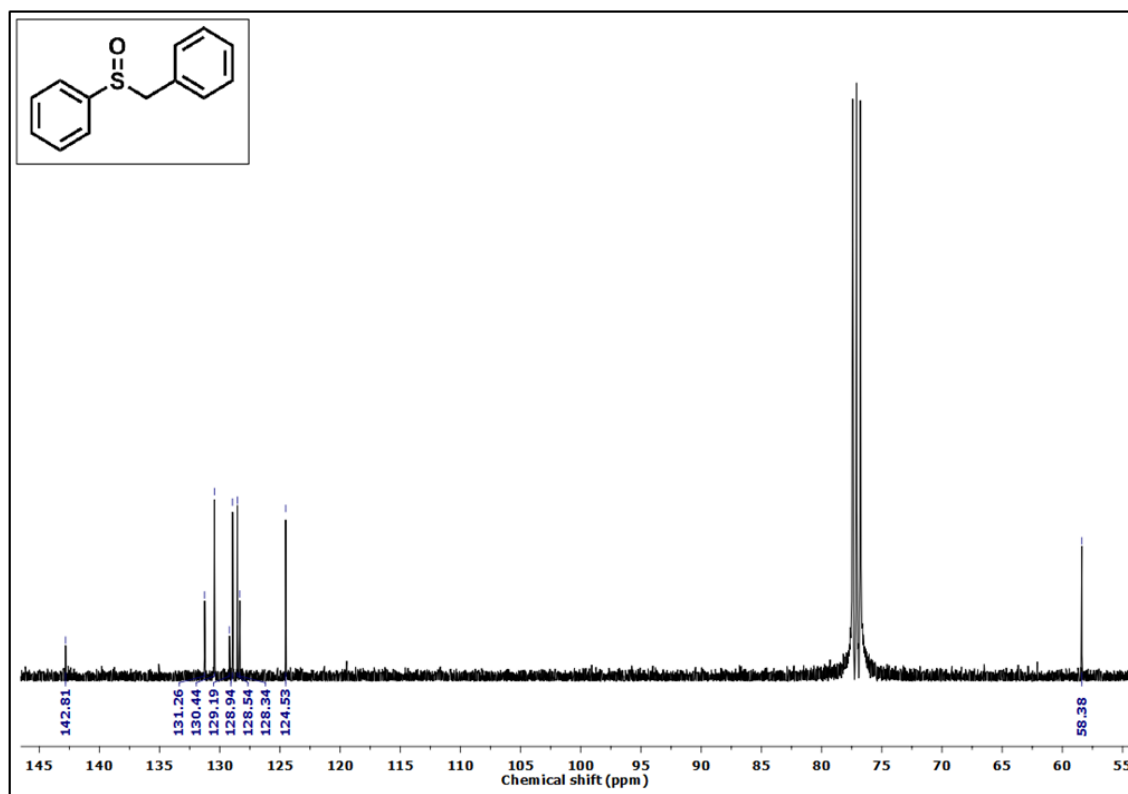
d)  $^{13}\text{C}$  NMR spectrum of diphenyl sulfoxide (**2b**)



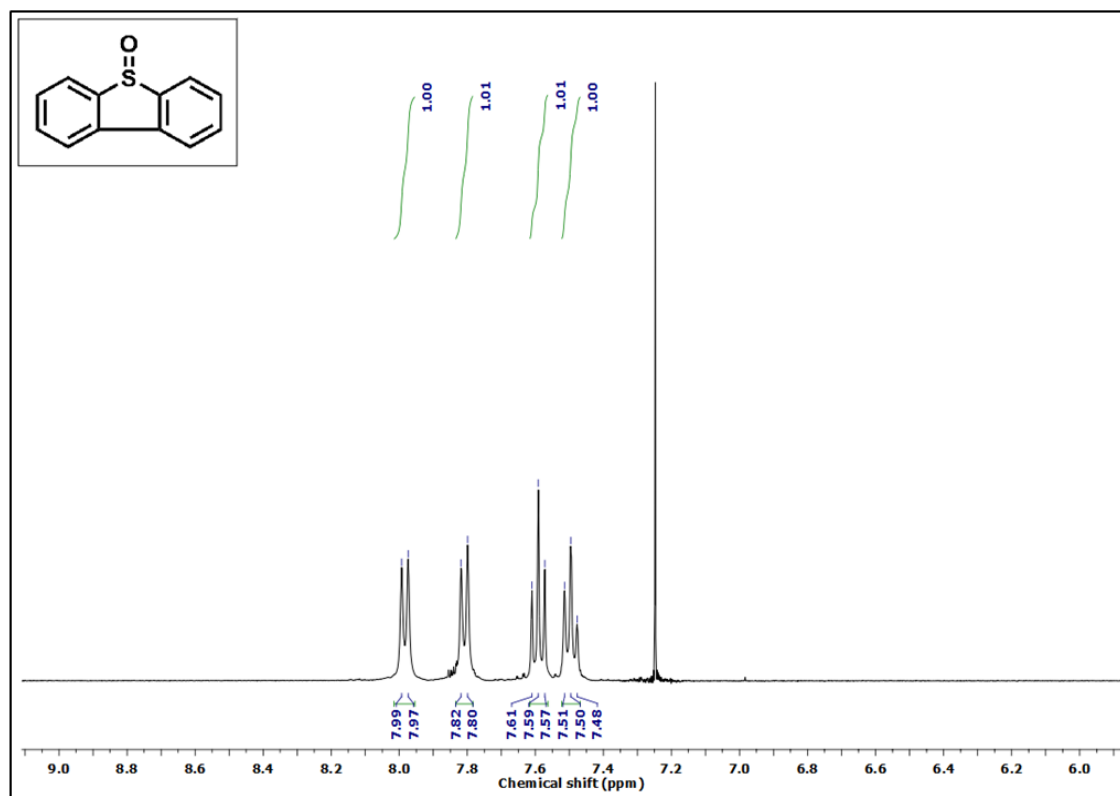
e)  $^1\text{H}$  NMR spectrum of benzyl phenyl sulfoxide (**2c**)



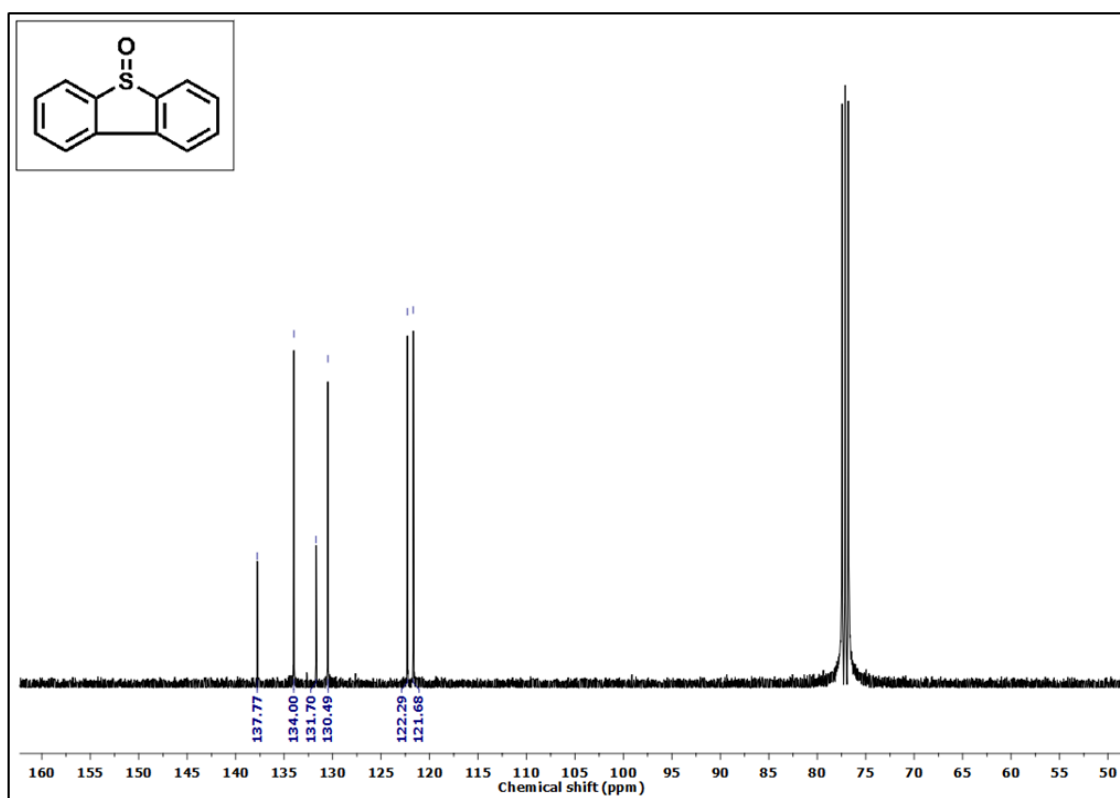
f)  $^{13}\text{C}$  NMR spectrum of benzyl phenyl sulfoxide (**2c**)



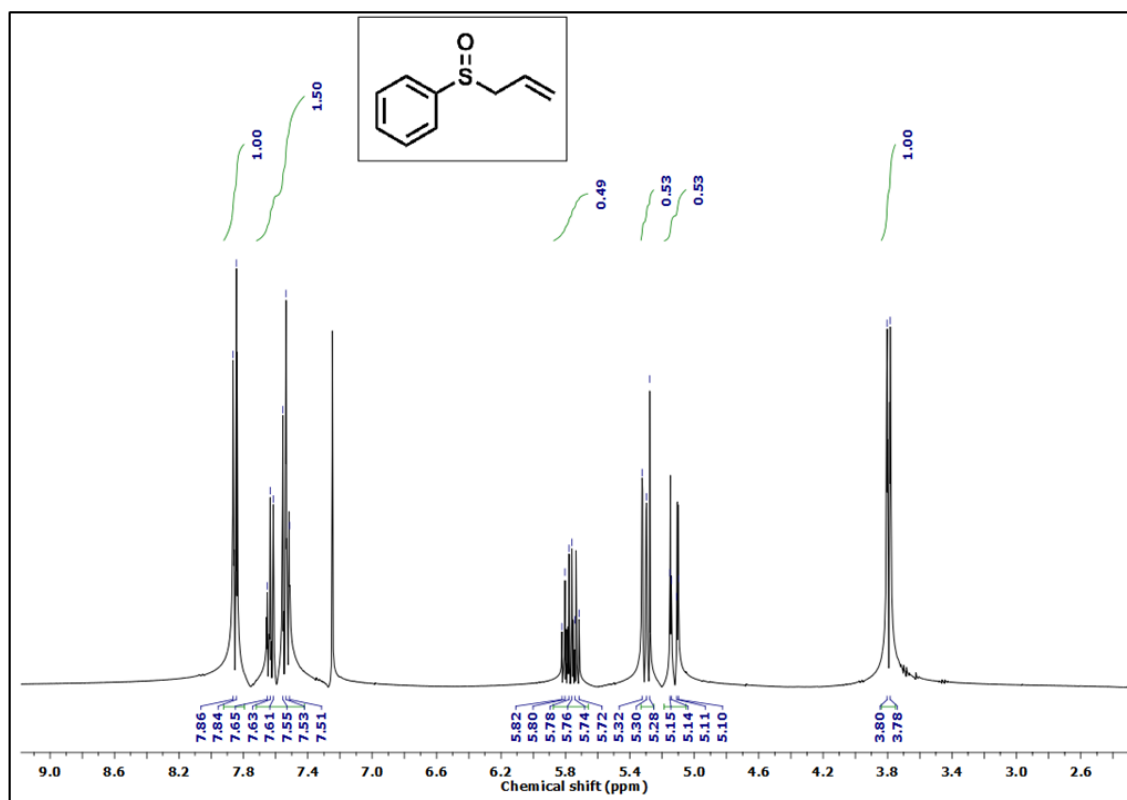
g)  $^1\text{H}$  NMR spectrum of dibenzothiophene-5-oxide (**2d**)



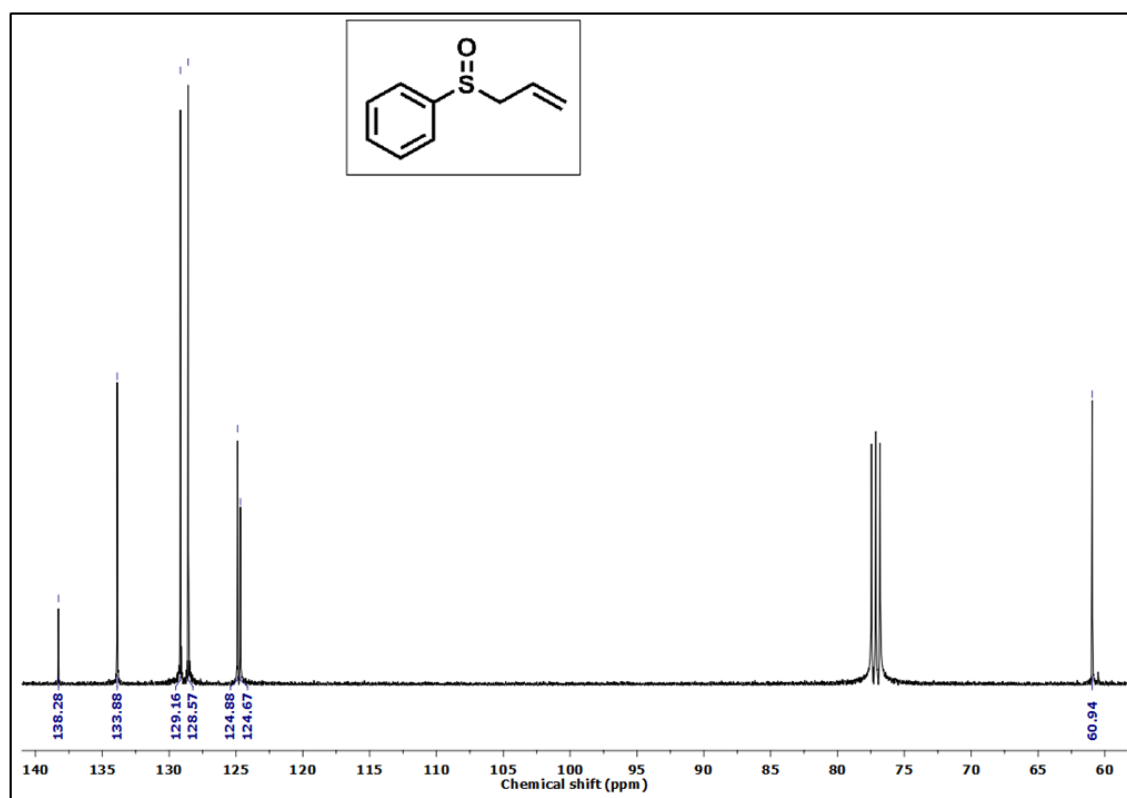
h)  $^{13}\text{C}$  NMR spectrum of dibenzothiophene-5-oxide (**2d**)



i)  $^1\text{H}$  NMR spectrum of allyl phenyl sulfoxide (**2e**)

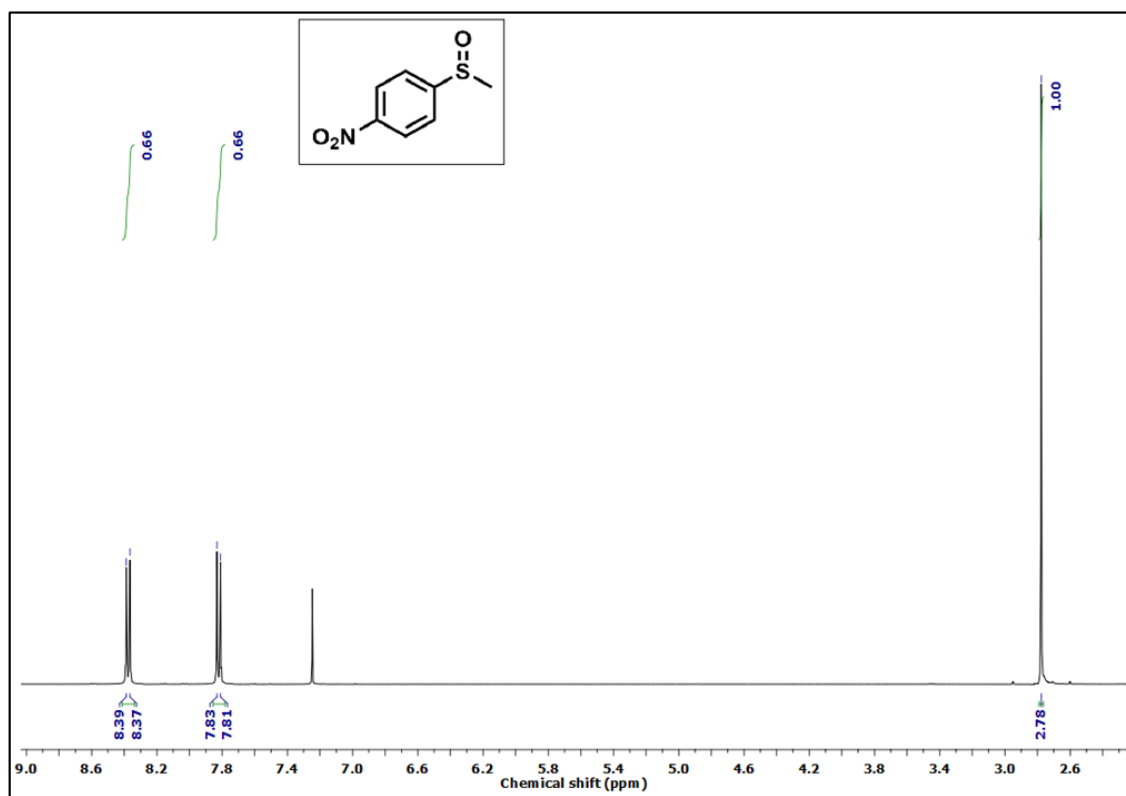


j)  $^{13}\text{C}$  NMR spectrum of allyl phenyl sulfoxide (**2e**)

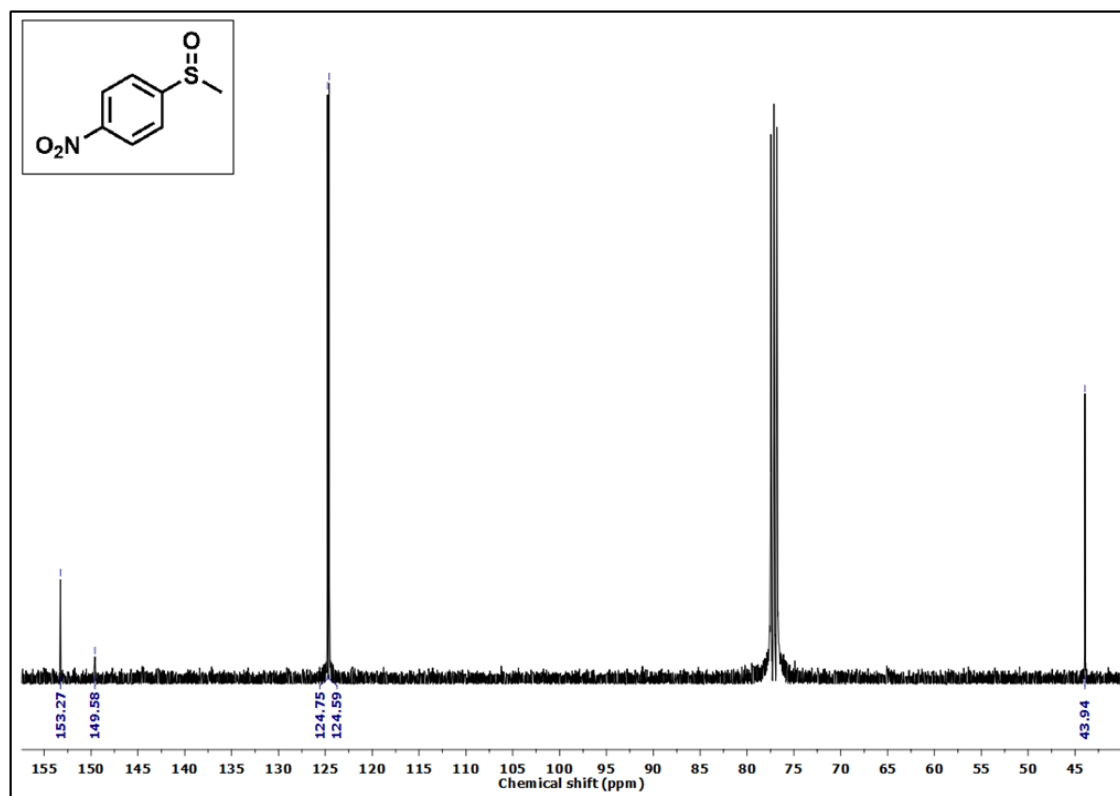




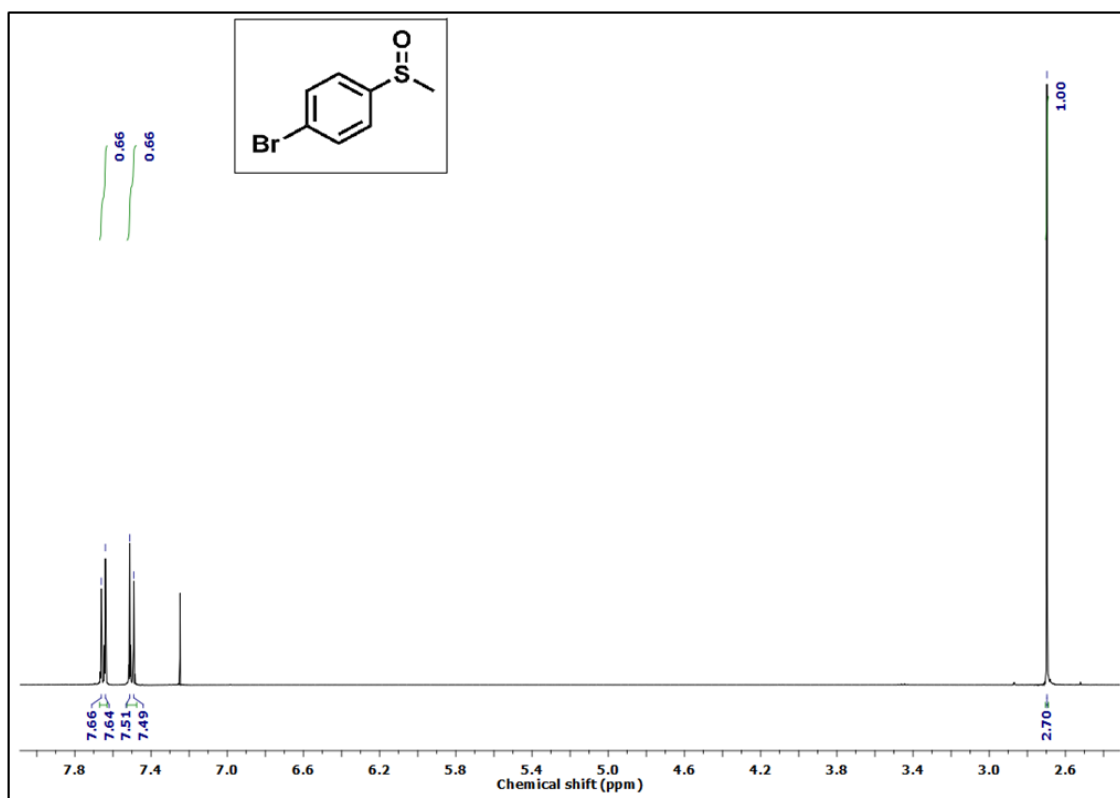
k)  $^1\text{H}$  NMR of methyl 4-nitrophenyl sulfoxide (**2f**)



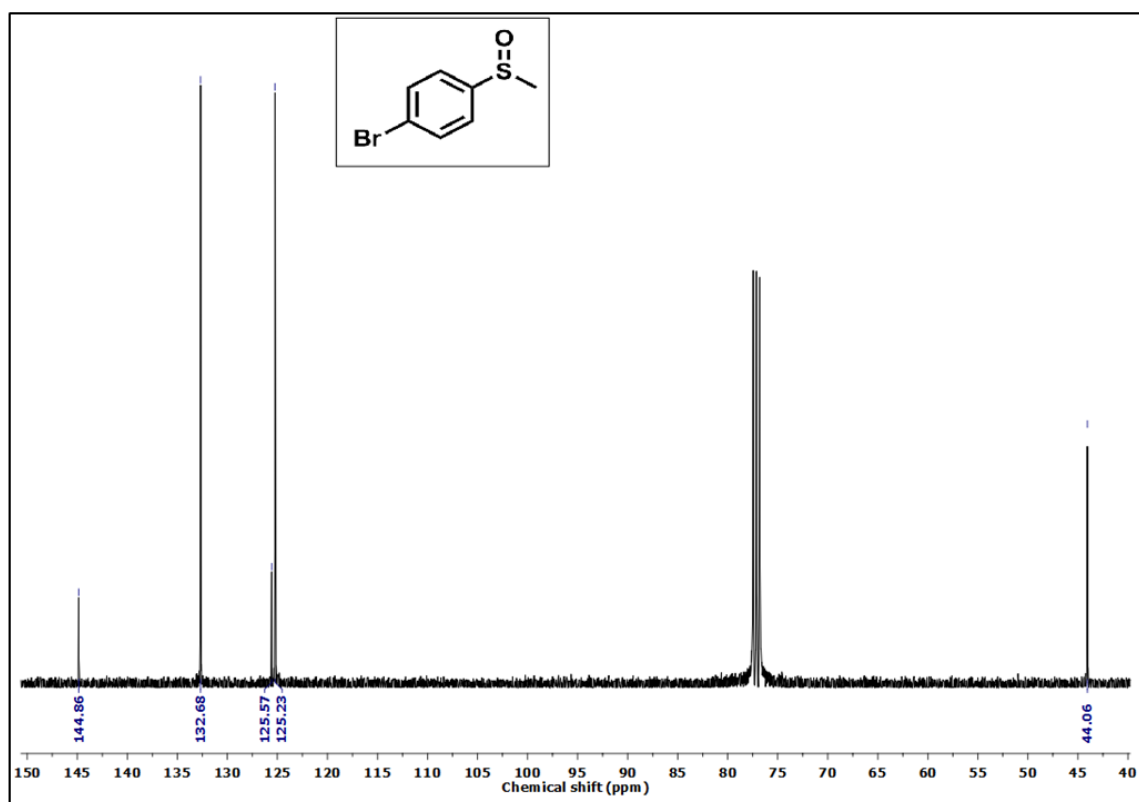
l)  $^{13}\text{C}$  NMR of methyl 4-nitrophenyl sulfoxide (**2f**)



m)  $^1\text{H}$  NMR of methyl 4-bromophenyl sulfoxide (**2g**)

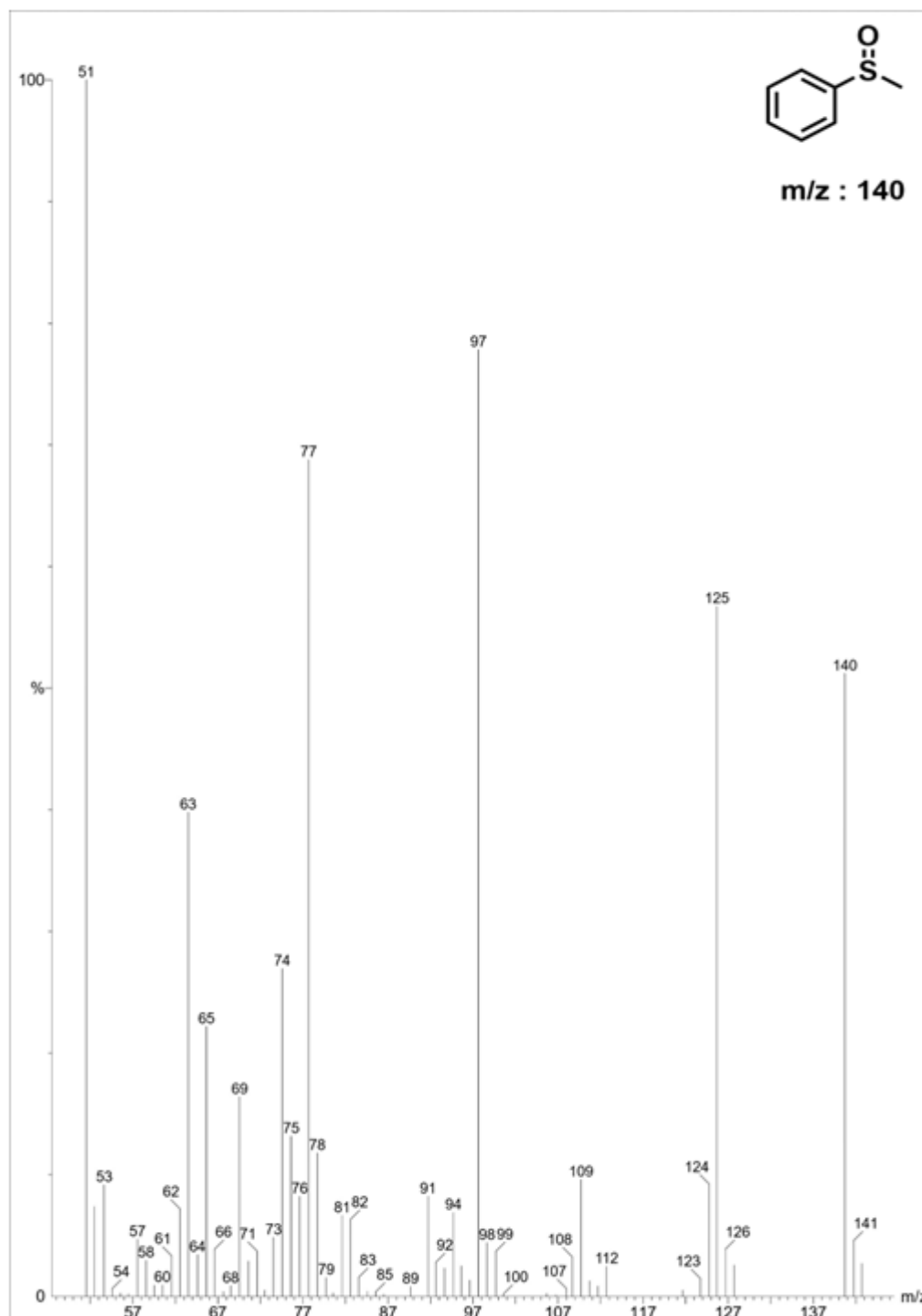


n)  $^{13}\text{C}$  NMR spectrum of methyl 4-bromophenyl sulfoxide (**2g**)

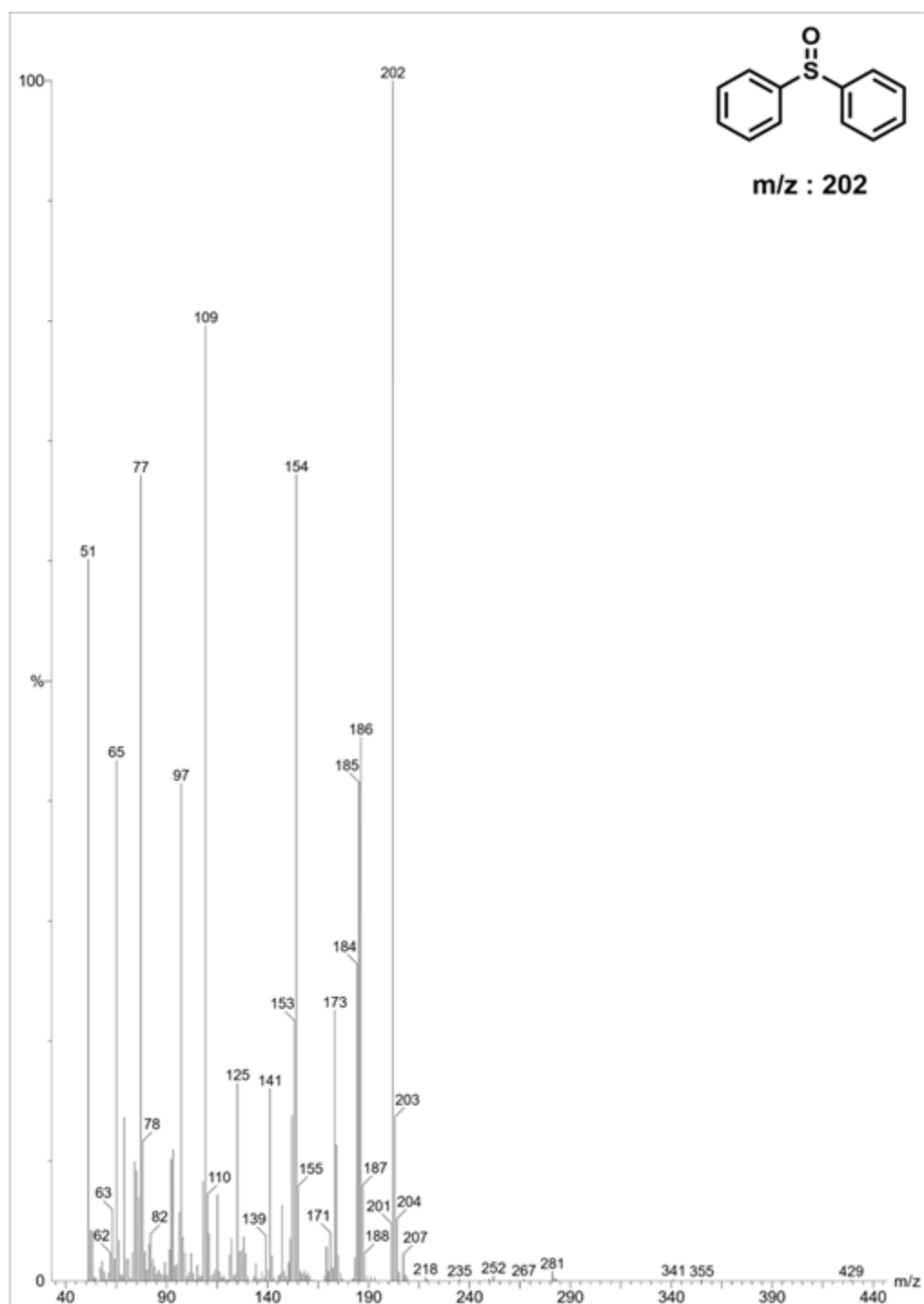


#### 4.4.8. Gas Chromatography-Mass Spectrometry spectra (GC-MS) of sulfoxide products

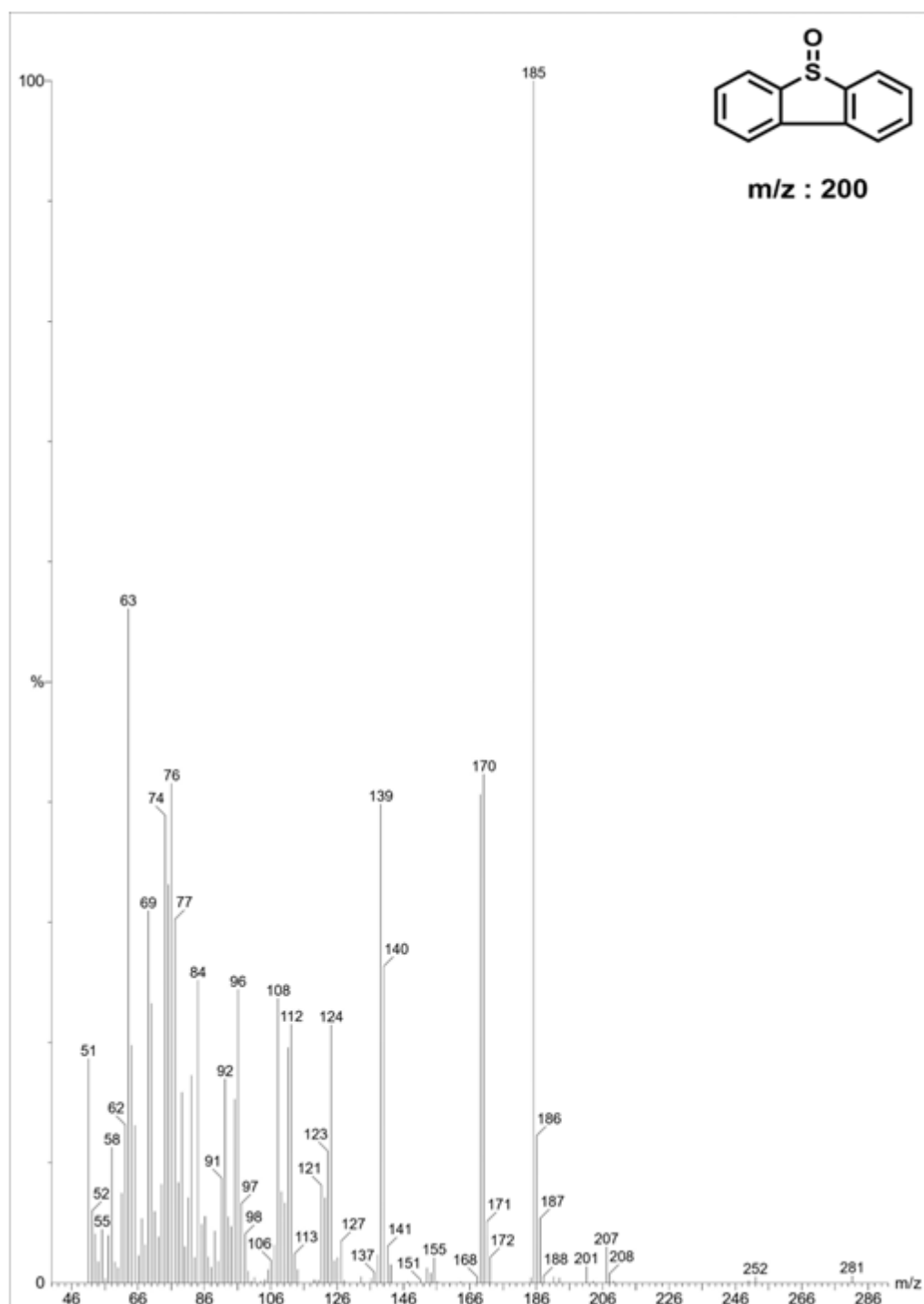
a) GC-MS spectrum of **2a**



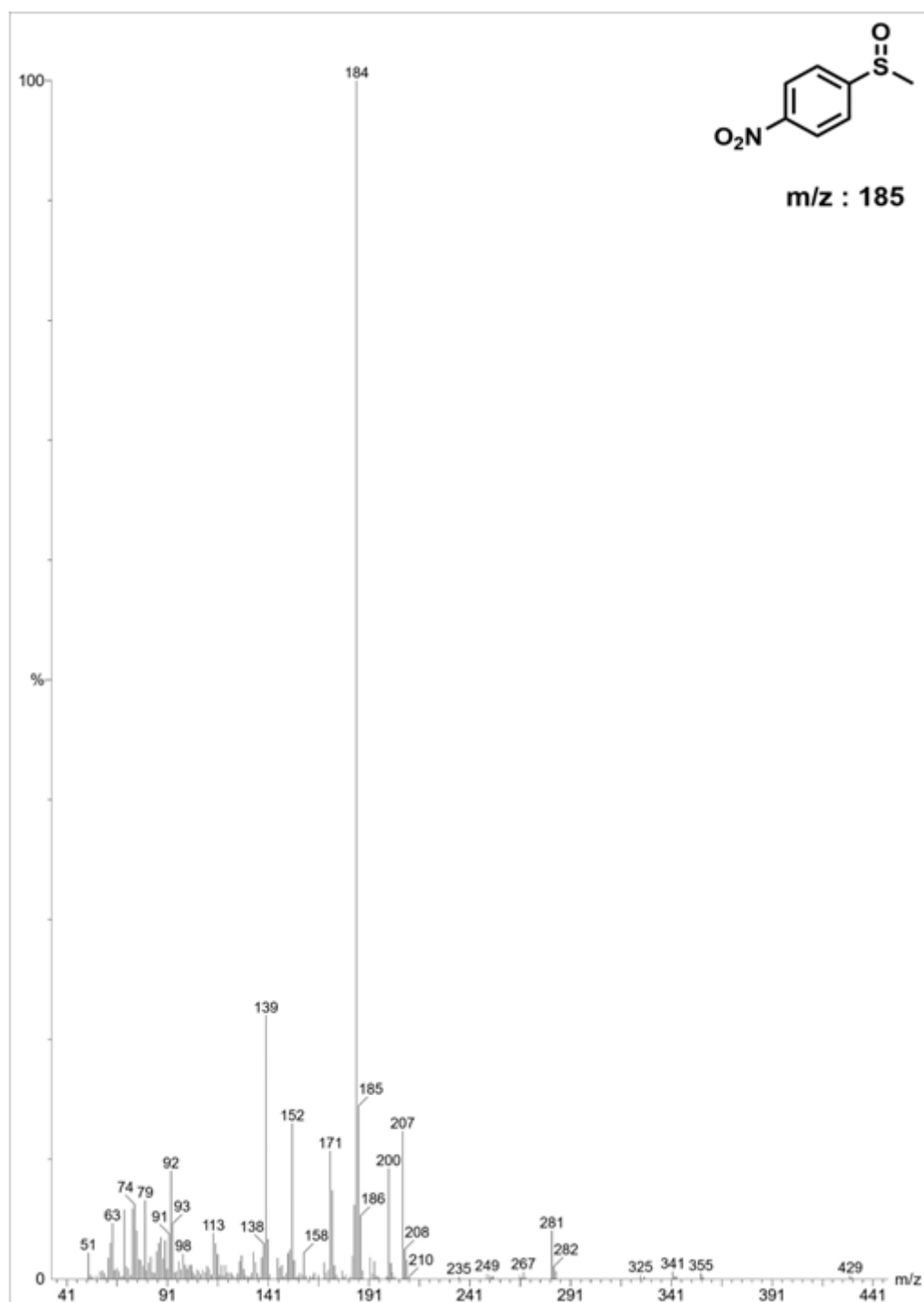
[m/z = 140 ( $M^+$ ), 125, 109, 98, 77, 63, 51 (100%)]

b) GC-MS spectrum of **2b**

[m/z = 202 ( $M^+$ , 100%), 186, 154, 125, 109, 77, 51]

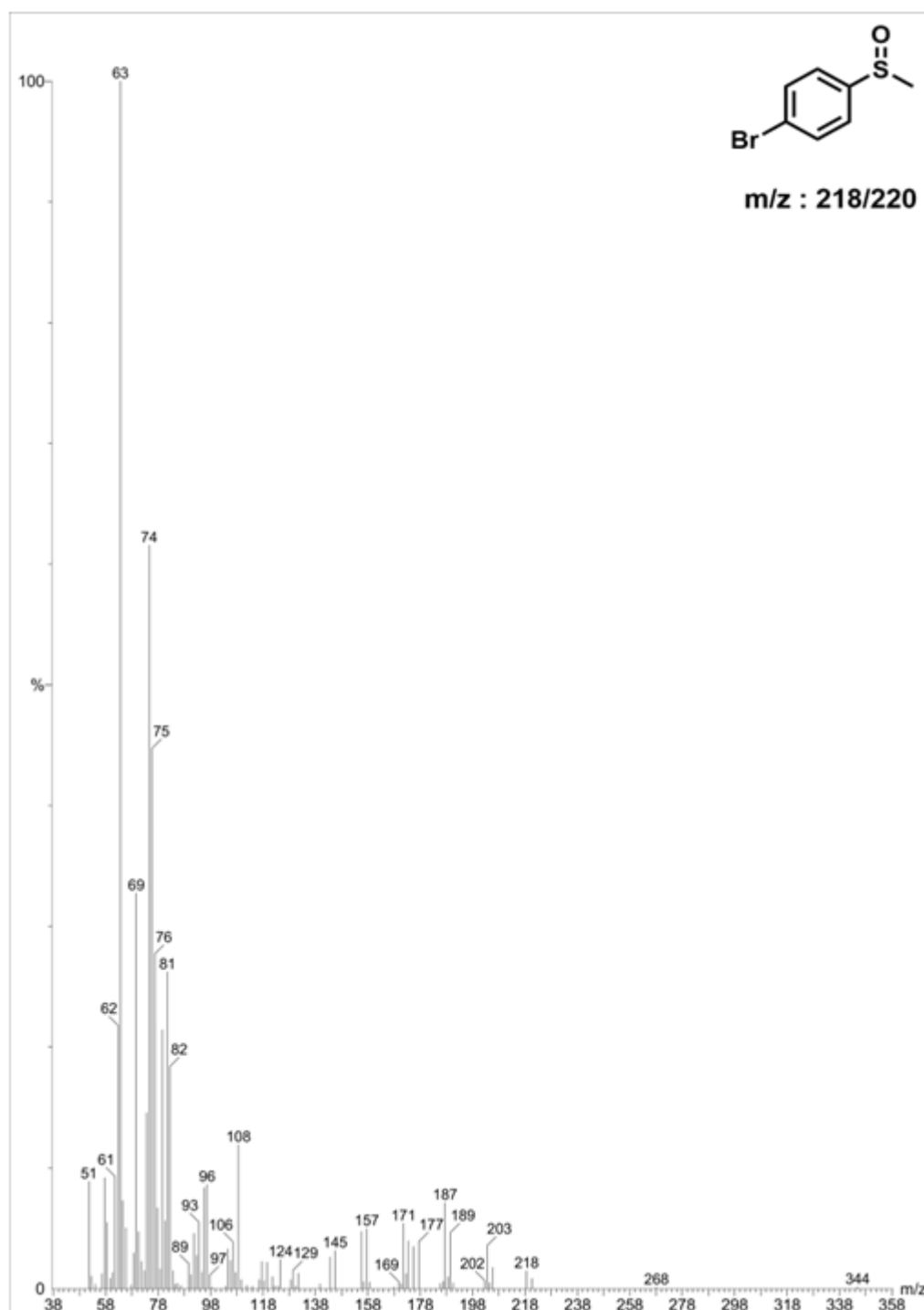
c) GC-MS spectrum of **2d**

[m/z = 201 ( $M+1^+$ ), 185 (100%), 170, 140, 124, 108, 96, 76, 63, 51]

d) GC-MS spectrum of **2f**

[m/z = 185 (M<sup>+</sup>), 184 (100%), 171, 158, 152, 139, 138, 113, 98, 91, 79, 63, 51]

e) GC-MS spectrum of **2g**



[m/z = 220 ( $M^+$ ), 218 ( $M^+$ ), 189, 187, 157, 155, 131, 129, 108, 91, 89, 81, 79, 76, 63, 51]



---

## 4.5. Bibliography

- [1] Capozzi, G., Patai, S., and Rappoport, Z. *The Syntheses of Sulphones, Sulfoxides and Cyclic Sulphides*. John Wiley & Sons, Chichester, New York, 1994.
- [2] O'Mahony, G. E., Ford, A., and Maguire, A. R. Asymmetric oxidation of sulfides. *Journal of Sulfur Chemistry*, 34(3):301-341, 2013.
- [3] Wojaczynska, E. and Wojaczynski, J. Enantioselective synthesis of sulfoxides: 2000– 2009. *Chemical Reviews*, 110(7):4303-4356, 2010.
- [4] Bentley, R. Role of sulfur chirality in the chemical processes of biology. *Chemical Society Reviews*, 34(7):609-624, 2005.
- [5] Fernández, I. and Khier, N. Recent developments in the synthesis and utilization of chiral sulfoxides. *Chemical Reviews*, 103(9):3651-3706, 2003.
- [6] Fascione, M. A., Adshead, S. J., Mandal, P. K., Kilner, C. A., Leach, A. G., and Turnbull, W. B. Mechanistic studies on a sulfoxide transfer reaction mediated by diphenyl sulfoxide/triflic anhydride. *Chemistry—A European Journal*, 18(10):2987-2997, 2012.
- [7] Carreño, M. C. Applications of sulfoxides to asymmetric synthesis of biologically active compounds. *Chemical Reviews*, 95(6):1717-1760, 1995.
- [8] Yang, C., Jin, Q., Zhang, H., Liao, J., Zhu, J., Yu, B., and Deng, J. Tetra-(tetraalkylammonium) octamolybdate catalysts for selective oxidation of sulfides to sulfoxides with hydrogen peroxide. *Green Chemistry*, 11(9):1401-1405, 2009.
- [9] Cotton, F. A. and Francis, R. Sulfoxides as ligands. I. A preliminary survey of methyl sulfoxide complexes. *Journal of the American Chemical Society*, 82(12):2986-2991, 1960.
- [10] Evans, D. A. and Andrews, G. C. Allylic sulfoxides. Useful intermediates in organic synthesis. *Accounts of Chemical Research*, 7(5):147-155, 1974.
- [11] Regueiro-Ren, A. Cyclic sulfoxides and sulfones in drug design. *Advances in Heterocyclic Chemistry*, 134:1-30, 2021.
- [12] Cai, S. Q., Zhang, K. F., and Cai, X. H. Recent advances in dimethyl sulfoxide (DMSO) used as a multipurpose reactant. *Current Organic Chemistry*, 26(2):91-121, 2022.
- [13] Xiang, J. C., Gao, Q. H., and Wu, A. X. The applications of DMSO. *Solvents as Reagents in Organic Synthesis: Reactions and Applications*, 315-353, 2017.

- 
- [14] Kwak, C., Lee, J. J., Bae, J. S., Choi, K., and Moon, S. H. Hydrodesulfurization of DBT, 4-MDBT, and 4, 6-DMDBT on fluorinated CoMoS/Al<sub>2</sub>O<sub>3</sub> catalysts. *Applied Catalysis A: General*, 200(1-2):233-242, 2000.
- [15] Shafi, R. and Hutchings, G. J. Hydrodesulfurization of hindered dibenzothiophenes: An overview. *Catalysis Today*, 59(3-4):423-442, 2000.
- [16] Ma, X., Sakanishi, K., and Mochida, I. Hydrodesulfurization reactivities of various sulfur compounds in diesel fuel. *Industrial & Engineering Chemistry Research*, 33(2):218-222, 1994.
- [17] Zhao, D., Wang, J., and Zhou, E. Oxidative desulfurization of diesel fuel using a Brønsted acid room temperature ionic liquid in the presence of H<sub>2</sub>O<sub>2</sub>. *Green Chemistry*, 9(11):1219-1222, 2007.
- [18] Kowalski, P., Mitka, K., Ossowska, K., and Kolarska, Z. Oxidation of sulfides to sulfoxides. Part 1: Oxidation using halogen derivatives. *Tetrahedron*, 61(8):1933-1953, 2005.
- [19] Shukla, V. G., Salgaonkar, P. D., and Akamanchi, K. G. A mild, chemoselective oxidation of sulfides to sulfoxides using o-iodoxybenzoic acid and tetraethylammonium bromide as catalyst. *The Journal of Organic Chemistry*, 68(13):5422-5425, 2003.
- [20] Kropp, P. J., Breton, G. W., Fields, J. D., Tung, J. C., and Loomis, B. R. Surface-mediated reactions. 8. Oxidation of sulfides and sulfoxides with tert-butyl hydroperoxide and oxone<sup>1</sup>. *Journal of the American Chemical Society*, 122(18):4280-4285, 2000.
- [21] Iranpoor, N., Firouzabadi, H., and Pourali, A. R. Dinitrogen tetroxide impregnated activated charcoal (N<sub>2</sub>O<sub>4</sub>/charcoal): Selective oxidation of sulfides to sulfoxides and disulfides to thiosulfonates. *Synlett*, 2004(02):0347-0349, 2004.
- [22] Zhang, B., Zhou, M. D., Cokoja, M., Mink, J., Zang, S. L., and Kühn, F. E. Oxidation of sulfides to sulfoxides mediated by ionic liquids. *RSC Advances*, 2(22):8416-8420, 2012.
- [23] Zhao, D., Wang, Y., Duan, E., and Zhang, J. Oxidation desulfurization of fuel using pyridinium-based ionic liquids as phase-transfer catalysts. *Fuel Processing Technology*, 91(12):1803-1806, 2010.
- [24] Liu, X. B., Rong, Q., Tan, J., Chen, C., and Hu, Y. L. Recent advances in catalytic oxidation of organic sulfides: Applications of metal–ionic liquid catalytic systems. *Frontiers in Chemistry*, 9:798603, 2022.
-

- 
- [25] Zhang, M., Zhu, W., Xun, S., Li, H., Gu, Q., Zhao, Z., and Wang, Q. Deep oxidative desulfurization of dibenzothiophene with POM-based hybrid materials in ionic liquids. *Chemical Engineering Journal*, 220:328-336, 2013.
- [26] Zhu, W., Li, H., Jiang, X., Yan, Y., Lu, J., and Xia, J. Oxidative desulfurization of fuels catalyzed by peroxotungsten and peroxomolybdenum complexes in ionic liquids. *Energy & Fuels*, 21(5):2514-2516, 2007.
- [27] Fareghi-Alamdari, R., Zekri, N., Moghadam, A. J., and Farsani, M. R. Green oxidation of sulfides to sulfoxides and sulfones with  $H_2O_2$  catalyzed by ionic liquid compounds based on Keplerate polyoxometalates. *Catalysis Communications*, 98:71-75, 2017.
- [28] Carrasco, C. J., Montilla, F., Álvarez, E., Mealli, C., Manca, G., and Galindo, A. Experimental and theoretical insights into the oxodiperoxomolybdenum-catalysed sulphide oxidation using hydrogen peroxide in ionic liquids. *Dalton Transactions*, 43(36):13711-13730, 2014.
- [29] Zhao, P., Zhang, M., Wu, Y., and Wang, J. Heterogeneous selective oxidation of sulfides with  $H_2O_2$  catalyzed by ionic liquid-based polyoxometalate salts. *Industrial & Engineering Chemistry Research*, 51(19):6641-6647, 2012.
- [30] P Bryliakov, K. and P Talsi, E. Transition metal catalyzed asymmetric oxidation of sulfides: from discovery to recent trends. *Current Organic Chemistry*, 16(10):1215-1242, 2012.
- [31] Leonard, N. J. and Johnson, C. R. Periodate oxidation of sulfides to sulfoxides. Scope of the reaction. *The Journal of Organic Chemistry*, 27(1):282-284, 1962.
- [32] Panda, M. K., Shaikh, M. M., and Ghosh, P. Controlled oxidation of organic sulfides to sulfoxides under ambient conditions by a series of titanium isopropoxide complexes using environmentally benign  $H_2O_2$  as an oxidant. *Dalton Transactions*, 39(9):2428-2440, 2010.
- [33] Gan, H. M., Qin, C., Zhao, L., Sun, C., Wang, X. L., and Su, Z. M. Self-assembled polyoxometalate-based metal-organic polyhedra as an effective heterogeneous catalyst for oxidation of sulfide. *Crystal Growth & Design*, 21(2):1028-1034, 2021.
- [34] Dash, S., Patel, S., and Mishra, B. K. Oxidation by permanganate: Synthetic and mechanistic aspects. *Tetrahedron*, 65(4):707-739, 2009.
-

- 
- [35] Bordwell, F. G. and Cooper, G. D. Conjugative effects of methylsulfonyl and methylthio groupings. *Journal of the American Chemical Society*, 74(4):1058-1060, 1952.
- [36] Banerji, K. K. Mechanism of the oxidation of organic sulphides by permanganate ion. *Tetrahedron*, 44(10):2969-2975, 1988.
- [37] Lee, D. G. and Chen, T. Oxidation of organic sulfides by permanganate ion. *The Journal of Organic Chemistry*, 56(18):5346-5348, 1991.
- [38] Shaabani, A., Tavasoli-Rad, F., and Lee, D. G. Potassium permanganate oxidation of organic compounds. *Synthetic Communications*, 35(4):571-580, 2005.
- [39] Jayaraman, A. and East, A. L. The mechanism of permanganate oxidation of sulfides and sulfoxides. *The Journal of Organic Chemistry*, 77(1):351-356, 2012.
- [40] Hajipour, A., Mallakpour, S., and Adibi, H. A facile and selective method for oxidation of sulfides and thiols to their corresponding sulfoxides and disulfides with alumina-supported potassium permanganate under solvent-free conditions. *Sulfur Letters*, 25(4):155-160, 2002.
- [41] Shaabani, A., Mirzaei, P., and Lee, D. G. The beneficial effect of manganese dioxide on the oxidation of organic compounds by potassium permanganate. *Catalysis Letters*, 97:119-123, 2004.
- [42] Shaabani, A., Rahmati, A., Sharifi, M., Rad, J. M., Aghaaliakbari, B., Farhangi, E., and Lee, D. G. Green oxidations. Manganese (II) sulfate aided oxidations of organic compounds by potassium permanganate. *Monatshefte für Chemie*, 138:649-651, 2007.
- [43] Shaabani, A., Bazgir, A., and Lee, D. G. Oxidation of organic compounds by potassium permanganate supported on montmorillonite K10. *Synthetic Communications*, 34(19):3595-3607, 2004.
- [44] Acharjee, A., Ali, M. A., and Saha, B. A review of the synthesis and utility of some lipophilic permanganate oxidants. *Journal of Solution Chemistry*, 47:1449-1478, 2018.
- [45] Schmidt, H. J. and Schäfer, H. J. Stability of benzyl (triethyl) ammonium permanganate. *Angewandte Chemie International Edition in English*, 18(10):787-787, 1979.
- [46] Scholz, D. New synthetic methods 4 1: Mild one-phase oxidation of sulfides and sulfoxides to sulfones. *Monatshefte für Chemie/Chemical Monthly*, 112:241-243, 1981.
-

- 
- [47] Paquette, L. A., Crich, D., Fuchs, P., Molander, G., Van Dyke, A. R., and Jamison, T. F. *Encyclopedia of Reagents for Organic Synthesis*. Wiley, Chichester, 2009.
- [48] Karaman, H., Barton, R. J., Robertson, B. E., and Lee, D. G. Preparation and properties of quaternary ammonium and phosphonium permanganates. *The Journal of Organic Chemistry*, 49(23):4509-4516, 1984.
- [49] Lakouraj, M. M., Tajbakhsh, M., Tashakkorian, H., and Ghodrati, K. Fast and efficient oxidation of sulfides to sulfones with N, N'-dibenzyl-N, N, N', N'-tetramethyl diammonium permanganate. *Phosphorus, Sulfur, and Silicon and the Related Elements*, 182(2):485-490, 2007.
- [50] Sarma, P., Dutta, A. K., and Borah, R. Design and exploration of -SO<sub>3</sub>H group functionalized Brønsted acidic ionic liquids (BAILs) as task-specific catalytic systems for organic reactions: A review of literature. *Catalysis Surveys from Asia*, 21:70-93, 2017.
- [51] Das, S., Kashyap, N., Kalita, S., Bora, D. B., and Borah, R. A brief insight into the physicochemical properties of room-temperature acidic ionic liquids and their catalytic applications in CC bond formation reactions. *Advances in Physical Organic Chemistry*, 54:1-98, 2020.
- [52] Giernoth, R. Task-specific ionic liquids. *Angewandte Chemie International Edition*, 49(16):2834-2839, 2010.
- [53] Singh, S. K. and Savoy, A. W. Ionic liquids synthesis and applications: An overview. *Journal of Molecular Liquids*, 297:112038, 2020.
- [54] Kashyap, N., Das, S., and Borah, R. Solvent responsive self-separation behaviour of Brønsted acidic ionic liquid-polyoxometalate hybrid catalysts on H<sub>2</sub>O<sub>2</sub> mediated oxidation of alcohols. *Polyhedron*, 196:114993, 2021.
- [55] Kalita, S., Kashyap, N., Bora, D. B., Das, S., and Borah, R. Investigation of N, N'-disulfopiperazinium chlorometallates of Fe (III), Ni (II) and Co (II) as hybrid catalysts for the synthesis of 1, 2-dihydroquinazoline derivatives. *ChemistrySelect*, 8(18):e202204533, 2023.
- [56] Dutta, A. K., Gogoi, P., and Borah, R. Diethyldisulfoammonium chlorometallates as heterogeneous Brønsted-Lewis acidic catalysts for one-pot synthesis of 14-aryl-7-(N-phenyl)-14H-dibenzo [a, j] acridines. *Applied Organometallic Chemistry*, 32(1):e3900, 2018.
- [57] Koodehi, T. G., Shirini, F., and Goli-Jolodar, O. Preparation, characterization and application of 1, 4-disulfopiperazine-1, 4-dium chloride ([Piper-(SO<sub>3</sub>H)<sub>2</sub>]<sup>+</sup>·2Cl<sup>-</sup>)
-

- as an efficient dicationic ionic catalyst for the N-Boc protection of amines. *Journal of the Iranian Chemical Society*, 14:443-456, 2017.
- [58] Khanna, R. K. and Stranz, D. D. Infrared and Raman spectra of  $\text{KMnO}_4$  complexed with 18-crown-6 ether. *Spectrochimica Acta Part A: Molecular Spectroscopy*, 36(4):387-388, 1980.
- [59] Hendra, P. J. The vibrational spectrum of the permanganate ion. *Spectrochimica Acta Part A: Molecular Spectroscopy*, 24(2):125-129, 1968.
- [60] Viste, A. and Gray, H. B. The electronic structure of permanganate ion. *Inorganic Chemistry*, 3(8):1113-1123, 1964.
- [61] Tanabe, I., Kurawaki, Y., Morisawa, Y., and Ozaki, Y. Electronic absorption spectra of imidazolium-based ionic liquids studied by far-ultraviolet spectroscopy and quantum chemical calculations. *Physical Chemistry Chemical Physics*, 18(32):22526-22530, 2016.
- [62] Engert, C. and Kiefer, W. Raman spectra of the permanganate ion in the solid state with excitation in the near infrared. *Journal of Raman Spectroscopy*, 22(11):715-719, 1991.
- [63] Hu, Y. L., Fang, D., and Xing, R. Efficient and convenient oxidation of sulfides to sulfoxides with molecular oxygen catalyzed by  $\text{Mn}(\text{OAc})_2$  in ionic liquid  $[\text{C}_{12}\text{mim}][\text{NO}_3]$ . *RSC Advances*, 4(93):51140-51145, 2014.
- [64] Hajipour, A. R., Khazdooz, L., and Ruoho, A. E. Selective and efficient oxidation of sulfides to sulfoxides using ceric ammonium nitrate (CAN)/Brønsted acidic ionic liquid. *Phosphorus, Sulfur, and Silicon and the Related Elements*, 184(3):705-711, 2009.
- [65] Hussain, S., Talukdar, D., Bharadwaj, S. K., and Chaudhuri, M. K.  $\text{VO}_2\text{F}(\text{dmpz})_2$ : A new catalyst for selective oxidation of organic sulfides to sulfoxides with  $\text{H}_2\text{O}_2$ . *Tetrahedron Letters*, 53(48):6512-6515, 2012.
- [66] Li, X. D., Ma, R., and He, L. N.  $\text{Fe}(\text{NO}_3)_3 \cdot 9\text{H}_2\text{O}$ -catalyzed aerobic oxidation of sulfides to sulfoxides under mild conditions with the aid of trifluoroethanol. *Chinese Chemical Letters*, 26(5):539-542, 2015.
- [67] Veerakumar, P., Lu, Z. Z., Velayudham, M., Lu, K. L., and Rajagopal, S. Alumina supported nanoruthenium as efficient heterogeneous catalyst for the selective  $\text{H}_2\text{O}_2$  oxidation of aliphatic and aromatic sulfides to sulfoxides. *Journal of Molecular Catalysis A: Chemical*, 332(1-2):128-137, 2010.